Riv. It. Peleont. Strat.	v. 92	n. 4	pp. 439–496	tav. 32–38	Marzo 1987

EVOLUTION OF THE TETHYS HIMALAYA CONTINENTAL SHELF DURING MAASTRICHTIAN TO PALEOCENE (ZANSKAR, INDIA)

ALDA NICORA *, EDUARDO GARZANTI* & ELISABETTA FOIS*

Key–words: Himalaya, India, Cretaceous, Paleocene, Stratigraphy, Foraminifera, Sandstone petrography, Anchimetamorphism, Sea–level changes, Passive margin.

Riassunto. La sequenza Maastrichtiano–Paleocenica dello Zanskar occidentale si è depositata sulla piattaforma continentale del margine passivo indiano, che andava gradualmente approfondendosi verso NE. La successione registra una tendenza generale regressiva alla fine del Cretaceo, quando l'abbassamento del livello marino a una velocità superiore al tasso di subsidenza causa dapprima un inquinamento terrigeno della rampa carbonatica di Marpo (*Siderolites* Beds) e quindi la migrazione della linea di costa verso l'oceano, con esposizione ed erosione di gran parte della piattaforma continentale.

La discordanza è poi ricoperta dalle quarzareniti di spiaggia di Stumpata, che indicano apporti terrigeni in equilibrio con una lenta risalita relativa del livello del mare nel Paleocene inferiore. La superficie di deposizione rimane sopra o vicina al raggio d'azione delle onde sia nella Falda di Zangla che nella Falda di Lingshed, che è caratterizzata da una monotona sequenza di isola–barriera. Al tetto della Quarzarenite di Stumpata, arenarie regressive fini e bioturbate sono seguite da un intervallo condensato, che testimonia una rapida trasgressione al termine del Paleocene inferiore.

Nel Paleocene superiore, la deposizione generalizzata di carbonati puri indica condizioni di alto livello marino senza apporti silicoclastici. Il Calcare di Dibling registra una tendenza regressiva, con passaggio ad ambienti di piattaforma interna da aperti a ristretti, testimoniata da faune e flore sempre meno diversificate e dominate verso l'alto da Alghe Udoteacee e Foraminiferi porcellanacei. Fino alla fine del Paleocene, il detrito silicoclastico è fornito alla piattaforma dello Zanskar da fiumi sub–equatoriali che drenano le piane costiere e il continente indiano posti a meridione, caratterizzati da moderato rilievo e da intensa alterazione pedogenetica in climi caldo–umidi.

Nell'Eocene inferiore, la progradazione di apparati deltizi alimentati dal margine asiatico settentrionale in via di obduzione segnerà poi la chiusura finale della Neotetide in Ladakh, con formazione di una catena montuosa proto–himalayana. La rapida transizione da margine passivo a catena in collisione è registrata anche dalla storia post–deposizionale della successione stratigrafica terziaria, che passò direttamente da una diagenesi superficiale durante la sedimentazione di margine passivo, a condizioni metamorfiche di grado molto basso sotto una copertura tettonica di circa 10 km, come risultato di una deformazione tangenziale con impilamento di falde durante l'orogenesi himalayana.

---

* Dipartimento di Scienze della Terra dell'Università degli Studi di Milano, Via Mangiagalli 34, 20133 Milano, Italy.

– E. Fois and A. Nicora worked out the biostratigraphy and microfacies of the Marpo and Dibling Limestones; E. Garzanti studied the petrography and sedimentology of the Stumpata Quartzarenite and is responsible for eustatic, diagenetic and geodynamic considerations. All authors made the survey in the field.

– Financial support from MPI 40%. Lithosphere Project "Geology of NW Himalaya–Karakorum".

Abstract. The results of several–year stratigraphic researches on the Northwestern Himalaya Late Cretaceous–Early Tertiary succession are here presented. New biostratigraphic data allowed to recognize several benthic foraminiferal assemblages in five measured stratigraphic sections and to reconsider the position of the Cretaceous–Tertiary boundary. Refined chronostratigraphic calibration and assessment of sedimentation rates were obtained through correlation between benthic and planktonic biozones. Petrographical analysis of sandstones allowed to tentatively put forward a sedimentological model, to give rough estimates for temperatures of anchimetamorphic deformation in the different thrust sheets of the Tethys Himalaya zone and to shed new light on the genesis of superstable and supermature quartzarenites. Integrated sedimentological–petrographical studies allowed to distinguish at least three depositional sequences separated by major unconformities in the previously undifferentiated succession, and to put further constraints to the dating of the India–Asia collision.

During the Maastrichtian, a regressive trend was marked by the northeastward progradation of the Marpo carbonate ramp on the outer neritic/upper bathyal Kangi La marls. The shallow–water Marpo Limestone was unconformably overlain by the coastal Stumpata Quartzarenite as a response to rapid sea–level fall close to the Cretaceous/Tertiary boundary. Highstand carbonate deposition resumed after a transgressive event in the mid–Paleocene, as testified by the Late Paleocene Dibling Limestone. Sedimentation was directly controlled by sea–level changes and siliciclastic detritus was supplied by northward–flowing sub–equatorial rivers, draining the low–relief and deeply–weathered Indian craton and coastal plains, until the end of the Paleocene, when tectonic uplift heralded the onset of the India–Eurasia continental collision. The passive margin sequence was then unconformably overlain by Eocene volcanic arenites, derived from the uplifted arc–trench systems of the Asian active margin and marking the final closure of the Neotethys Ocean. During the Himalayan orogeny, the Tertiary Zanskar sequence underwent anchimetamorphic fold–thrust deformation at temperatures between at least 250° and 300° C under a tectonic load of several kilometers.

Introduction.

The present paper represents a synthesis of the researches carried out by members of the «Dipartimento di Scienze della Terra, Università degli Studi di Milano» on the Late Cretaceous–Tertiary sequence of Zanskar Range (Ladakh, Himalaya) during three expeditions from 1977 to 1984 (Gaetani et al., 1980, 1983, 1985a; Baud et al., 1984). While in the two first expeditions (1977, 1981) only the lower and middle/upper portions of the sequence were studied in the Kanji (1) (Gaetani et al., 1980) and Spanboth (Gaetani et al., 1983) sections, in the last one (1984) also its uppermost part was investigated in two sections (Marpo and Dibling). A brief summary on the data from these two sections has been already published in Gaetani et al. (1985a). Further observations about the regional context of the sequence have been collected by one of us (E.G.) during an expedition (1983) carried out with A. Baud (Lausanne) and G. Mascle (Grenoble).

According to recent structural interpretations (Bassoullet et al., 1983; Baud et al., 1984; Gaetani et al., 1985b), the Zanskar synclinorium consists of several superposed thrust sheets (Zangla, Lingshed and Shillakong Nappes (fig. 1, 2 in Gaetani et al., 1985b), tectonically transported towards the SW. The

(1) We use the term Kanji for the topographic name as published in the Ladakh–Zanskar map (Pegasus Ed., 1983), whereas the term Kangi designates the formation name as originally proposed by Fuchs (1982).

latter authors also recognized a ramp structure at Pingdon La which separates a Lower from an Upper Zangla Nappe. These two distinct thrust–sheets have undergone different metamorphic deformation, as documented herein by petrographic evidence.

This paper mostly deals with the inner shelf succession of Late Cretaceous –Paleocene age of the Zangla Nappe. The mainly shelf–slope sedimentary sequence of the Lingshed Nappe will be discussed in a forthcoming paper (Baud et al., in preparation).

The Latest Cretaceous to Paleocene sequence of the Zanskar Range, comprised between the Late Cretaceous outer shelf/slope Kangi La marls and the Eocene Chulung La fluviodeltaic red beds, has been designated as Spanboth Formation by Fuchs (1982). Gaetani et al. (1983, 1985a) and Baud et al. (1984) used this formation name with the same meaning but subdivided the Spanboth Fm. in three distinct members: a lower member mostly calcareous with abundant *Omphalocyclus*; a middle member predominantly arenaceous with subordinate hybrid arenites and an upper member, calcareous, rich in *Daviesina* in its lower portion. Detailed studies on five sections, measured in different tectonic units (Fig. 1), allowed us to recognize in Fuchs' Spanboth Fm. a composite succession consisting of at least three distinct depositional sequences,

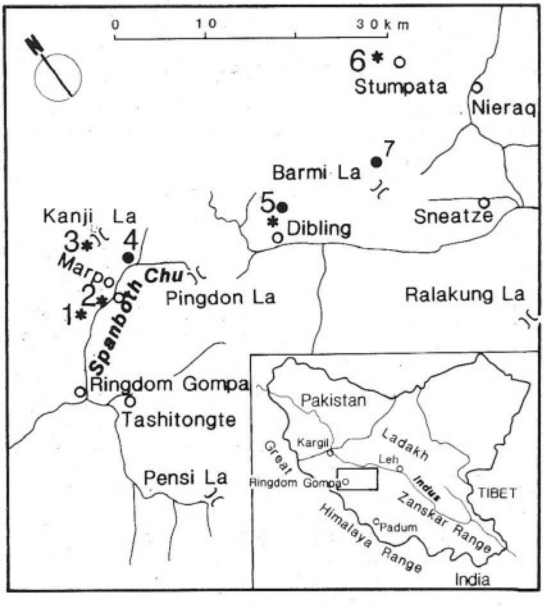

Fig. 1 – Location map of the studied western Zanskar area. Asterisks and dots respectively indicate measured stratigraphic sections referred to in the text and surveyed outcrops. 1) Spanboth; 2) Marpo; 3) Kanji; 4) Upper Spanboth Valley, E of Marpo; 5) Dibling; 6) Stumpata; 7) Barmi La.

FORMATION	LITHOZONE	SAMPLES	LITHOLOGY	SEDIMENTARY STRUCTURES	MICROFACIES	BIOFACIES	AGE
DIBLING LIMESTONE	C	HZ 330 HZ 326	Light grey—greenish silty clays and subordinate intercalations of dark bioclastic calcilutites and fine calcarenites (21 m). At the base alternations of dark clays and planar dark grey calcilutites (4 m)		Bioclastic wackestones to packstones with abundant micrite. Locally diffuse clay fraction. Few silicified bioclasts	Dominant benthic foraminifers (miliolids, rotaliids, *Chrysalidinae*, *Textulariidae*, *Orbitolites* sp., *Fasciolites* sp.). Rare ostracods	LATE PALEOCENE
	B	HZ 325	Planar dark grey bioclastic calcilutites and marly calcilutites and subordinate light planar bioclastic calcarenites (54 m). Up to HZ 325		Bioclastic wackestones to packstones with abundant micrite	Dominant benthic foraminifers (miliolids, rotaliids, *Fasciolites* (*G.*) *subtilis* (Hottinger), *F.* (*G.*) *levis* (Hottinger), *F. avellana* (Hottinger), *F. cucumiformis* (Hottinger). Rare ostracods	
			Planar, grey, fine bioclastic calcarenites alternating to greenish—grey to dark marly calcilutites and clays (11 m). Up to HZ 315		Bioclastic wackestones. Mud chips	Benthic foraminifers (miliolids, rotaliids, *Chrysalidinae*, *Textulariidae*, *Valvulinidae*, *Operculina* sp.)	
		HZ 311	Planar ligh grey to brownish bioclastic calcilutites. In one layer round white calcite bodies (36 m). Up to HZ 313	Strong bioturbation in the calcilutites.	Bioclastic wackestones. Diffuse clay. Quartz extraclasts	Dominant benthic foraminifers (miliolids, *Textulariidae*, *Chrysalidinae*, rotaliids, *Daviesina khatiyahi* Smout, *D. langhami* Smout, *Operculina* sp., *Orbitolites* sp.).Very rare dasycladacean *Algae*	
	A	HZ 310 HZ 308	Dark grey nodular calcilutites with locally lenses of bioclasts (76 m). At the base few clay intercalations		Bioclastic wackestones to packstones with abundant micrite	Abundant benthic foraminifers (rotaliids, *Chrysalidinae*, miliolids, *Textulariidae*, *Daviesina danieli* Smout, *D. khatiyahi* Smout, *D. langhami* Smout, *Ranikothalia* sp., *Operculina* sp., *Orbitolites* sp.). Subordinate dasycladacean *Algae* (*Clypeina* cf. *merienda* Elliott, *Furcoporella diplopora* Pia, *Trinocladus* sp.), rare udoteacean *Algae* (*Ovulites* sp., *O.* cf. *kangpensis* Yu—Jing). Very rare corallinacean *Algae*	
		HZ 307 HZ 306				Abundant benthic foraminifers (rotaliids, miliolids, *Ataxophragmiidae*, *Chysalidina* sp.). Subordinate dasycladacean *Algae* (*Furcoporella* cf. *diplopora* Pia, *Clypeina* cf. *merienda* Elliott)	LATE EARLY PALEOCENE
		HZ 305	White to dark grey sandstones alternating to dark clays and siltstones. In the uppermost 8 m dark, planar to nodular marly calcilutites are intercalated with dark clays and marly clays (21 m)		Limestones: bioclastic mudstones/ wackestones, rarely packstones. Diffuse clay fraction	Udoteacean *Algae* (*Ovulites* sp.), ostracods, rare pelecypods, benthic foraminifers (miliolids, rotaliids, *Lockhartia* sp.)	
			Bottom not exposed				

Table 1 — Lithology and biostratigraphic content in the Marpo section.

FORMATION	LITHOZONE	SAMPLES	LITHOLOGY	SEDIMENTARY STRUCTURES	MICROFACIES	BIOFACIES	AGE
DIBLING LIMESTONE	C	HZ 408 HZ 413	Grey–greenish clays and silty clays with intercalations of marly limestones and planar to slightly nodular bioclastic calcarenites, locally in lenses (31 m)	Fine cross laminations. Local bioturbation	Bioclastic packstones, subordinate wackestones. Locally abundant peloids. Clay fraction	Dominant benthic foraminifers (miliolids, rotaliids, *Lockhartia* sp., textulariids, *Chrysalidinae*, *Orbitolites* sp., *Fasciolites* (*G.*) *levis* (Hottinger), *F.* gr. *ellipsoidalis* (Schwager). Diffuse udoteacean *Algae* (*Ovulites* cf. *margaritula* (Lamarck), *O.* cf. *elongata* Lamarck, rare *Halymeda lingulata* Yu–Jing). Ostracods, subordinate echinoderms, gastropods	EOCENE
	B	HZ 414 HZ 422	Planar to slightly nodular amalgamated, grey fine bioclastic calcarenites. Locally black chert nodules (38 m)	Bioturbation	Bioclastic packstones with abundant micrite. Locally quartz extraclasts	Dominant benthic foraminifers (miliolids, textulariids, *Chrysalidinae*, *Ataxophragmiidae*, *Fasciolites* (*G.*) *subtilis* (Hottinger), *F.* (*G.*) *levis* (Hottinger), *F. avellana* (Hottinger), *F. cucumiformis* (Hottinger), *F.* gr. *ellipsoidalis* (Schwager), *Lockhartia* sp., *Orbitolites* sp.). Locally abundant udoteacean *Algae* (*Ovulites* cf. *margaritula* (Lamarck), *O.* cf. *elongata* Lamarck, *Halymeda lingulata* Yu–Jing). Echinoderms, ostracods	LATE PALEOCENE
			Tectonic repetition of Lithozone B (partially) and Lithozone C				
	C	HZ 407 HZ 403	Greenish to grey–dark grey clays and marly clays. Thin silty–sandy layers. At the base thin intercalation of bioclastic calcarenites. Towards the top bioclastic marly calcilutites/fine calcarenites (34 m)	Cross and convolute laminations into the silty–sandy layers	Bioclastic wackestones to packstones with abundant micrite. Clay fraction. Fine quartz extraclasts	Benthic foraminifers (miliolids, textulariids, rotaliids, *Orbitolites* sp., *Fasciolites* sp.). Udoteacean *Algae* (*Ovulites* cf. *elongata* Lamarck, *O.* cf. *margaritula* (Lamarck). Ostracods, echinoderm fragments	
	B	HZ 402	Thin bedded dark grey bioclastic calcilutites and marly limestones. Topmost part made of amalgamated dark grey bioclastic calcarenites (14 m). Up to HZ 402		Bioclastic wackestones to packstones	Very abundant benthic foraminifers (miliolids, *Chrysalidinae*, *Ataxophragmiidae*, *Textulariidae*, *Fasciolites* (*G.*) *subtilis* (Hottinger), *F.* (*G.*) *levis* (Hottinger), *F. avellana avellana* (Hottinger), *F. a. aurignacensis* (Hottinger), *F. cucumiformis* (Hottinger), *F.* cf. *ellipsoidalis* (Schwager), *Orbitolites* sp., *Lockhartia* sp.). Very abundant udoteacean *Algae* (*Ovulites* cf. *elongata* Lamarck, *O.* cf. *margaritula* (Lamarck), *Halymeda lingulata* Yu–Jing). Echinoderms, ostracods, gastropods	
			Planar amalgamated dark grey coarse to fine bioclastic calcarenites (75 m). Up to HZ 397	Bioturbation	Bioclastic wackestones (lower part) to packstones (upper part)	Dominant benthic foraminifers (Miliolidae, *Chrysalidina*, *Ataxophragmiidae*, *Fasciolites* sp.). Subordinate echinoderms, ostracods, udoteacean *Algae* (*Ovulites* cf. *elongata* Lamarck)	
...STONE		HZ 386	Marly calcilutites with bioclasts. Characterististic horizon rich in Ostreids. Subordinate bioclastic calcarenites ([illegible] m). Up to HZ [illegible]	Cross lamination. Bioturbation	Bioclastic wackestones Bioclastic packstones; medium energy	Ostreids; benthic foraminifers (miliolids, rotaliids). Dominant echinoderms; benthic foraminifers (miliolids, *Textulariidae*, *Ataxophragmiidae*, *Chrysalidinae*, *Fasciolites* sp.). Rare bryozoans	...ENE

DIBLING LIME[illegible]	A	HZ 385	Nodular dark grey bioclastic calcilutites embedded in dark grey marls (26 m). Up to HZ 385		Bioclastic peloidal packstones with abundant micrite	Benthic foraminifers (miliolids, *Chrysalidinae*, *Lockhartia*, sp., *Daviesina khatiyahi* Smout, *D. langhami* Smout, *Orbitolites* sp., *Ranikothalia* sp., *Operculina* sp., *Sphaerogypsina* sp.). Rare corallinacean *Algae* (*Corallina* sp., *Jania* sp., *Distichoplax biserialis* (Dietrich). *Fasciolites* (*G.*) *primaeva* (Reichel) is present in sample HZ 382	LATE PALEOC[illegible]
			Planar amalgamated dark grey bioclastic calcilutites; local dolomitization; black chert nodules (9 m). Up to HZ 380		Bioclastic wackestones	Benthic foraminifers (miliolids, *Chrysalidinae*, *Orbitolites* sp., *Daviesina khatiyahi* Smout, *D. langhami* Smout, *Ranikothalia* sp., *Sphaerogypsina* sp.)	
		HZ 374	Nodular dark grey bioclastic calcarenites embedded in dark grey marls. Thick intercalation of grey marls (24 m). Up to HZ 378	Strong bioturbation	Bioclastic wackestones to packstones with abundant micrite	Benthic foraminifers (miliolids, *Chrysalidinae*, *Rotalia* sp., *Lockhartia* sp., *Daviesina danieli* Smout, *D. khatiyahi* Smout, *Orbitolites* sp., *Operculina* sp., *Sphaerogypsina* sp.). Rare ostracods, echinoderms	
		HZ 373	Planar to slightly nodular dark grey bioclastic calcilutites and fine calcarenites with intercalations of dark grey marls (12 m). Up to HZ 373		Bioclastic wackestones	Dominant benthic foraminifers (miliolids, *Chrysalidinae*, rotaliids, *Rotalia* sp., *Lockhartia* sp.). Rare udoteacean *Algae* (*Ovulites* cf. *elongata* (Lamarck) and dasycladacean *Algae* (*Cymopolia* sp., *Furcoporella* cf. *diplopora* Pia). Rare gastropods, pelecypods	LATE EARLY PALEOCENE
STUMPATA QUARTZARENITE		HZ 369 HZ 362	Planar lenticular, light sandstones (qz very abundant) (30 m). Up to HZ 369. The topmost 5 m are dark grey sandstones with an intercalation of dark clays	Amalgamated thickening–upwards sequences; normal grading; clay chips. Bioturbation at the base of one sequence. Parallel and cross lamination			EARLY ? PALEOCENE
MARPO LIMESTONE	SIDEROLITES Beds	HZ 361	Dark clays with few intercalations of planar light sandstones (qz very abundant) (10 m). Up to HZ 361				LATE MAASTRICHTIAN
			Lens–shaped bioclastic calcarenites with sandy seams (5 m). Up to HZ 359–360		Bioclastic packstones with abundant micrite	Dominant crinoids. Benthic foraminifers (*Siderolites calcitrapoides* Lamarck, *Omphalocyclus macroporus* (Lamarck)	
		HZ 356	Planar, white sandstones (qz very abundant) intercalated with dark clays (8 m). Up to HZ 358	Bioturbation onto the upper surface of the sandstone layers			
	OMPHALOCYCLUS Beds	HZ 355	Grey marls and dark clays with intercalations of grey bioclastic calcarenites. Fairly abundant crinoids remains (20 m).Up to HZ 355	Diffuse bioturbation (Zoophycos) in the marls	Bioclastic packstones. Low medium energy	Bryzoans, echinoderms, pelecypods, gastropods, udoteacean *Algae* (*Arabicodium* sp.), benthic foraminifers (miliolids, *Fissoelphidium* sp., *Goupillaudina* sp., *Gavelinella* sp., *Omphalocyclus macroporus* (Lamarck)	
		HZ 344	Slightly nodular to planar, thin bedded, grey calcilutites and thin marly intercalations. Fairly abundant whole echinoids (22 m). Up to HZ 349	Strong bioturbation (Zoophycos)	Bioclastic mudstones. Abundant quartz extraclasts	Benthic foraminifers (miliolids, *Textulariidae*, *Gavelinella* sp.)	

Table 2 – Lithology and biostratigraphic content in the Dibling section.

separated by unconformities, which are from bottom to top: the Marpo Limestone, the Stumpata Quartzarenite and the Dibling Limestone.

For detailed descriptions of the whole sequence in the Spanboth and Kanji sections the reader can refer to Gaetani et al. (1980, 1983). Detailed descriptions of each formation from the Marpo and Dibling sections are reported in Tab. 1, 2 respectively. On Tab. 5, 6 the fossil range charts of the Dibling and Marpo sections are indicated; in Gaetani et al. (1980 and 1983) the fossil range charts of the Kanji and Spanboth sections can be found. Further data on the sedimentary sequence of the Lingshed area, characterized by Maastrichtian offshore pelites (Goma and Kubar La Formations) and by Paleocene deep–water carbonates (Shinge La Limestone) followed by shallow–water nummulitic limestones (Kesi Formation) and marine pelites (Kong Formation), will be presented in a forthcoming paper (Baud et al., in preparation).

The Late Cretaceous–Tertiary sequence of the Zanskar shelf is very rich in age–diagnostic fossils (Gaetani et al., 1980, 1983, 1985a). The fossil content is dominated by large, well diversified benthic foraminifers (Fig. 14), Algae, corals, oysters. The biozonation of the sequence is based especially on the fossil content from the Dibling section, where sampling was particularly closely spaced. Cross–checking and comparisons with the other sections helped to better define the biostratigraphic succession. Based on the fossil content 11 assemblage zones have been identified. Two of them belong to the Late Cretaceous, eight cover most of the Paleocene and one marks the Paleocene–Eocene boundary.

Marpo Limestone.

We introduce the new name Marpo Limestone to designate the carbonate succession sedimented between the Kangi La Formation and the arenaceous unit here denominated Stumpata Quartzarenite. The appropriate name would have been Spanboth Limestone, but according to the International Stratigraphic Guide (Hedberg Ed., 1976, chapt. 5, G, 2), the name Spanboth, already used by Fuchs (1982), is no more available. Close to Marpo (Fig. 1, 9), the Late Cretaceous–Paleocene succession crops out and it represents a lateral continuation of the sequence studied in the Spanboth Chu section by Gaetani et al. (1983). The Marpo Limestone corresponds to the lower portion of Fuchs' Spanboth Fm., to the Lower Member of the Spanboth Fm. of Gaetani et al. (1983, 1985a), Baud et al. (1984) and to levels 1, 2 (= *Omphalocyclus* Beds) and 3 of Gaetani et al. (1980). We assume as its type–section the succession corresponding to the Lower Member of the Spanboth Fm. in the Spanboth Chu section of Gaetani et al. (1983).

Lithology.

The Marpo Limestone has been studied in three measured sections (Fig. 2): Spanboth (140 m), Kanji (160 m) and Dibling (68 m). It is subdivided into the *Zoophycos, Omphalocvclus* and *Siderolites* Beds which are defined after their

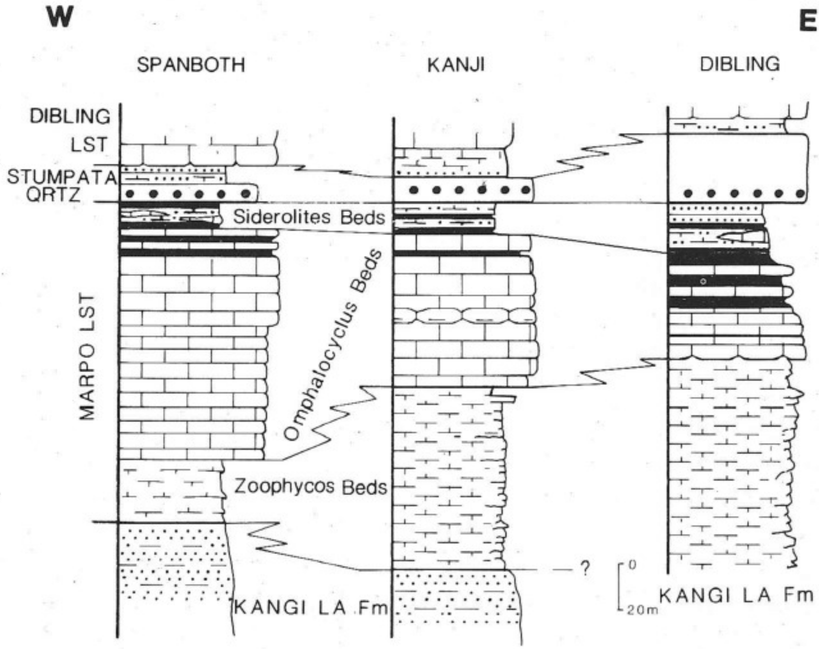

Fig. 2 – The Marpo Limestone and its members in the Spanboth, Kanji and Dibling sections.

fossil content, for fossils in these units are major physical constituents and for the lack of suitable geographic names. From bottom to top:

1) *Zoophycos* Beds: dark grey calcareous siltites and marls in poorly defined beds, rich in *Zoophycos* and *Rhizocorallium* burrows. At Spanboth, dark grey marly limestones (mudstones/wackestones, subordinate floatstones) in packed beds (20–30 cm thick) alternated with thin–bedded siltites and marls make up the upper part (11.5 m). This interval represents the transition to the underlying Kangi La Formation. It has been recognized only in the Spanboth (28.5 m thick) and Kanji (80 m thick) sections, whereas at Dibling it cannot be separated from the uppermost marls of the Kangi La Fm.

2) *Omphalocyclus* Beds: this lithozone is characterized by the common occurrence of *Omphalocyclus macroporus* (Lamarck). The lower portion consists of dark grey, slightly nodular limestones (10–30 cm thick beds) amalgamated to form thicker beds (30–60 cm thick). Nodules are encased in yellowish, brown weathered marls and siltites. This facies is present at Dibling (mostly bioclastic mudstones with abundant quartz extraclasts; 5.2 m thick, samples HZ 344–345) and Kanji, where it is thicker (wackestones to packstones and subordinate grainstones; 37 m thick), while at Spanboth it was not observed. Grey or dark grey planar and medium–bedded (20–30 cm thick) marly limestones follow with thin marly intercalations (bioclastic packstones/wackestones, grainstones especially at Kanji). In the upper part marly intercalations become frequent. Marls prevail at Dibling (samples HZ 349–355) (Fig. 2), where the upper portion of the *Omphalocyclus* Beds is characterized by about 20 m of grey to dark grey marls and clays with thin (20 cm thick) intercalations of grey bioclastic calcarenites. The uppermost part consists of 3.8 m of grey, brown weathered biocalcarenites (bioclastic packstones) capped by 3 m of black clays.

The latter unit represents most of the formation at Spanboth (102 m thick); whilst it is 65.3 m thick at Kanji and 42 m at Dibling.

3) *Siderolites* Beds: it is a characteristic pelitic interval at the top of the Marpo Limestone, increasing in thickness towards the east. It consists of 10.7 m thick grey siltstones and marls at Spanboth and of about 15 m of poorly exposed grey calcareous pelites at Kanji. At Dibling, the *Siderolites* Beds are 23 m of brown, moderately well sorted and very fine grained sandstones with feeding burrows, interbedded with dark pelites and bioclastic packstones (HZ 356 to 361). *Siderolites calcitrapoides* Lamarck characterizes the upper part of this lithozone at Spanboth (HZ 147) and Dibling (HZ 359, 360). At Kanji, abundant *Siderolites calcitrapoides* have been found in sample H 5, which was collected in the periglacial cover and thus it is considered not in place.

The thickness and carbonate content of the Marpo Limestone characteristically decrease from west to east (Fig. 2). The boundary with the underlying Kangi La Formation is transitional for some tens of meters and it was placed at the beginning of «skeletal carbonate grains within the quartzose siltite sequence» of the Kangi La Fm. (Gaetani et al., 1983).

The faunal content does not vary across this transitional boundary, and an association characterized by *Omphalocyclus macroporus* (Lamarck) was found in the Dibling section both in the upper portion of the Kangi La Fm. (HZ 342–343) and in the Marpo Limestone (HZ 344) (Fig. 14). The upper boundary with the Stumpata Quartzarenite is sharp and marked by the sudden appearance of fine–medium quartzarenites and by the disappearance of carbonate sediments.

Fossil content and age.

The Marpo Limestone is characterized by the abundant occurrence of *Omphalocyclus macroporus* (Lamarck) in all of the studied sections (*Omphalocyclus macroporus* Assemblage A, present paper). This well known species is generally associated with small foraminifera (miliolids, textulariids and *Lagenidae*), corals, crinoids. *Iraquia* cf. *complanata* Henson (= *Dictyoconella*), *Pseudorbitolina* sp., *Kilianina* sp., *Minouxia* sp. are especially developed in the Kanji section, where a very rich floral content (Assemblage B of Gaetani et al., 1980) consisting of abundant *Dasycladaceae (Acroporella, Cymopolia, Trinocladus)* and rarer *Corallinaceae (Archaeolithothamnium)* is also present. In the Dibling section, the Marpo Limestone is characterized by the presence of *Goupillaudina* sp. A few specimens of the same species were also found in the upper part of the Kangi La Fm. (HZ 343).

The upper part of the Marpo Limestone is characterized by *Siderolites calcitrapoides* Lamarck (Assemblage B, present paper). This assemblage, almost monospecific in the Spanboth (HZ 147) and Kanji (H 5) sections, is particularly well represented in the Dibling section (HZ 359, 360) where the index–species is associated with large *Omphalocyclus macroporus* (Lamarck), small foraminifera (*Gavelinella* sp., textulariids, miliolids), ostracods, echinoderms and corals.

A and B Assemblages present almost the same fossil content in all the investigated sections. Depending on diagenesis and metamorphism the fossil preservation is more or less good in the different sections. A new finding is the presence of representatives of *Goupillaudina* (A Assemblage) in the Dibling section since the upper part of the Kangi La Fm. where also *Omphalocyclus macroporus* (Lamarck) is present. As already pointed out (Gaetani et al., 1980, 1983) *Orbitoides* and *Lepidorbitoides* are absent, environmental conditions are accounted.

The costant common presence of *Omphalocyclus macroporus* (Lamarck) in the whole Marpo Limestone and the occurrence of *Siderolites calcitrapoides* Lamarck in its uppermost portion point to a Maastrichtian age for the unit and possibly to a Late Maastrichtian age for its top.

Depositional environment.

The Marpo Limestone is interpreted as a shallow–water carbonate ramp deposit diversified from inner infralittoral (Spanboth) to a deeper area (Kanji), while at Dibling outer shelf conditions are testified. It represents a regressive trend (northeastward progradation) with increasing of terrigenous pollution in its upper part (very fine grained sandstones in the *Siderolites* Beds) because of a progressive lowering of base level.

Stumpata Quartzarenite.

Close to the Cretaceous/Tertiary boundary, the sedimentary succession of the Zangla Nappe is characterized by a thin quartzarenite marker–horizon, which was considered by Gaetani et al. (1983, 1985a) as the Middle Member of the Spanboth Formation (Fuchs, 1982). This interval has been recently confirmed to be time–correlative with the quartzarenites forming the base of Fuchs' (1982) Lingshed Limestone in the Lingshed Nappe (Baud et al., 1985). In order to avoid cumbersome nomenclature, the formal name of «Stumpata Quartzarenite», after the thickest section measured in the 1983 expedition above the villages of Stumpata and Goma, is here proposed to designate this arenaceous unit in the whole Zanskar.

Lithology.

The Stumpata Quartzarenite was studied at the type–locality in the Lingshed Nappe and in four stratigraphic sections, belonging to the Lower (Spanboth, Marpo) and Upper (Kanji, Dibling) Zangla thrust sheets (Fig. 1). Observations were made along a 40 km WNW–ESE geological transverse, roughly 45° oblique with respect to the original depositional strike, which ran about NNW–SSE.

In the 13 m thick Spanboth section, 6 m thick, white, thick–bedded and fine grained quartzarenites (HZ 148) are followed by a poorly exposed sequence of burrowed grey sandstones passing from thin bedded and very fine grained (HZ 149, 150) to fine grained (HZ 151). The formation is closed by immature, poorly sorted and fine grained bioclastic quartzarenites containing large ostreid shells (HZ 152), followed by texturally inverted beds with ferruginous peloids and crab remains (HZ 152b), and then by micritic wackes with bivalves and echinoderm fragments (HZ 153). A very similar 10 m thick sequence, capped by oxidized sandy layers with phosphatic clasts and overlain by inner shelf carbonates of the Dibling Limestone, was measured at Marpo.

In the Kanji section, 9.6 m thick grey to white, fine to medium grained quartzarenites (H 6) underlie several metres of silty marls followed by dark grey fossiliferous packstones. The quartzarenites gradually thicken toward the NE. About 20–25 m thick, vertically stacked, cross–laminated sandstone bodies showing lateral accretion bedding, were observed E of Marpo (Fig. 3). Cross–beds dip eastward and are replaced laterally by thinner arenaceous layers.

In the Dibling section, 30 m thick clean quartzarenites (HZ 362 to 369) are arranged in several progradation (thickening– and coarsening–upward) cycles (Fig. 4). Cycles consist of thin and lenticular beds of burrowed or laminated, fine grained sandstones locally with dark pelitic intraclasts up to 5 ÷ 10 cm in size, passing upward to white, thick–bedded and lower medium grained sandstones with high–angle tangential cross–lamination. Tabular sets of cross–laminae suggest bidirectional paleocurrents (NE–ward and subordinately W–ward). Vertical dwelling burrows were observed. The uppermost part of the unit consists of 5 m thick, grey, burrowed and fine grained sandstones (HZ 368, 369) with intercalated dark pelites, capped by subrounded immature, poorly sorted and fine grained quartzarenites with *sharp* basal contact (HZ 370). The latter layer yielded rotaliid foraminifera (*Lockhartia* sp.), and is followed by the open inner shelf Dibling Limestone.

The quartzarenitic body reaches a thickness of 67 m at Stumpata, where it sharply overlies about 30 m of grey marls. The quartzarenites are white to grey, fine grained, often cross–laminated and sporadically bioturbated (Q 62 to Q 51). Tabular or subordinately

Fig. 3 – Cross–bedded multistory sandstone bodies E of Marpo are interpreted as mainly meandering tidal channel deposits in backbarrier settings. Single sigmoidal units in lateral accretion bedding may represent normal intertidal sediments, separated by erosional surfaces scoured in higher energy periods (De Mowbray, 1983).

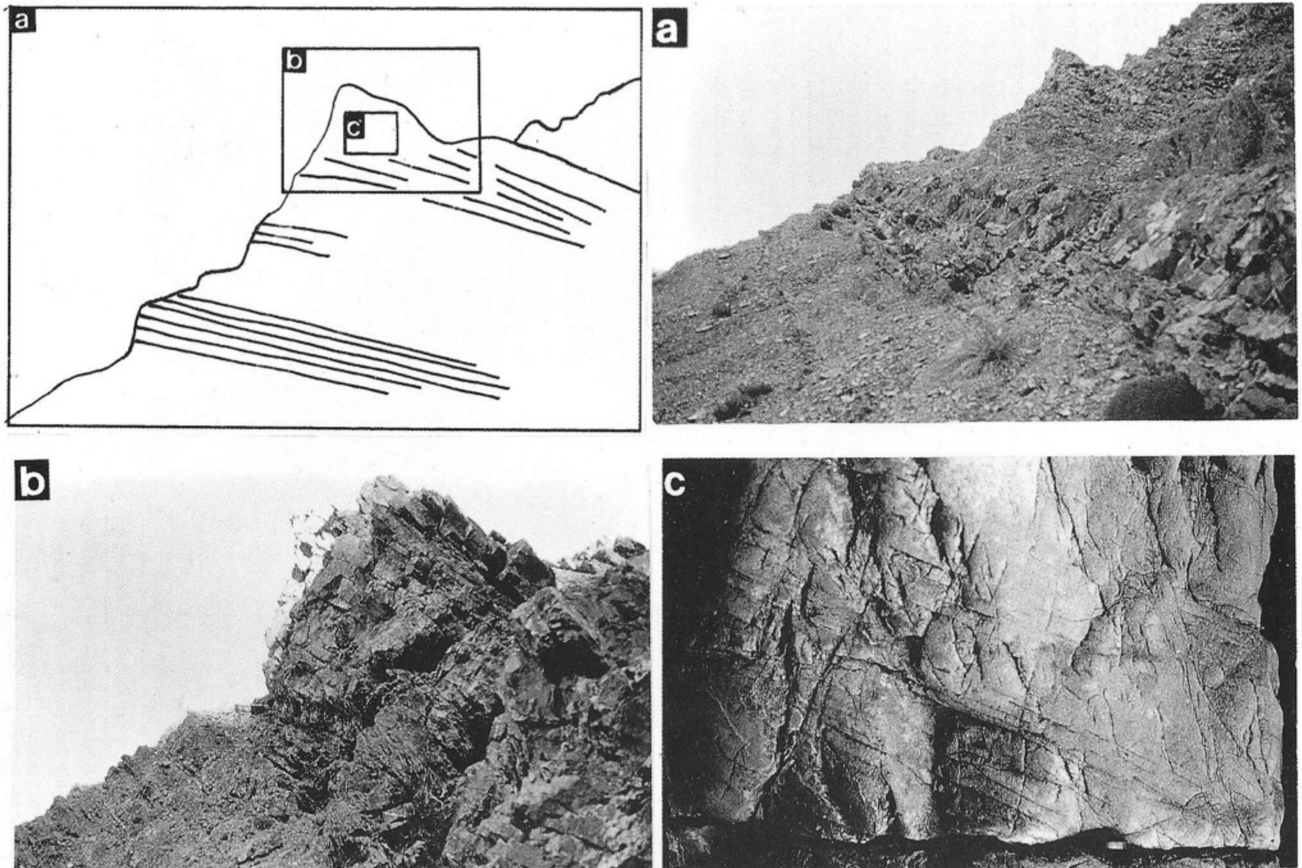

Fig. 4 – The Dibling section consists of several superposed progradation cycles capped by lower medium grained quartz-arenites (a). A closer picture (b), shows a well–developed shoaling sequence containing tabular sets of high–angle angular cross–lamination in its middle–upper part, as shown in detail (c). Seaward dip of cross–laminae may be ascribed to deposition under the action of ebb tidal currents.

lenticular, frequently amalgamated beds 20 to 100 cm thick locally show poorly defined thickening–upward cycles. The upper 19 m of the Stumpata sequence consist of calcareous sandstones and siltstones, sharply followed by the Shinge La pelagic limestones (Baud et al., 1985).

The Stumpata Quartzarenite abruptly overlies the *Siderolites* Beds, a pelitic interval considered as the uppermost part of the Marpo Limestone. The unit consists of clean sandstones in the lower part («Main quartzarenite body»), which increases eastward in thickness from 6 m at Spanboth to 67 m at Stumpata (Fig. 5), overlain by darker, finer grained and burrowed sandstones («Upper quartzarenites»). At the top of the formation, texturally inverted layers containing glaucony peloids and phosphatic clasts or Paleocene foraminifera may testify to reduced sedimentation rates («Condensed interval»).

Petrography.

Textures. The main body of the Stumpata Qzt. is made of fine to lower medium–grained and well to moderately sorted clean quartzarenites (Folk, 1980). Coarser grains may be up to perfectly spherical and rounded. Grain size distribution is almost invariably bimodal (except for finer–grained sandstones, which lack the coarse mode), and many samples may be described as bimodally supermature (Folk, 1980, p. 103). The fine mode occurs in the fine sand range and is generally moderately well sorted, whereas the coarse mode, occurring in the upper medium sand range, is mostly moderately sorted. Both the coarse mode and maximum grain size tend to decrease from Dibling, where medium grained sandstones are common, to Stumpata, where average grain size is restricted to the 200 ÷ 250 μm range, reflecting truncation of the coarse tail in the transport direction (Table 3). Clean sandstones are generally coarse skewed and platykurtic, but these primary depositional features may be masked by introduction of «matrix» due to organic activity, and burrowed samples are leptokurtic and fine skewed («poorly washed»). The muddy samples at the top of the formation have a third grain size mode in the fine silt to clay range (Table 4). Textural inversion phenomena

STRATIGR. SECTIONS	Average Size Φ	Longest Axis Φ	Grain size Modes Φ	Sorting σΦ	Range Φ units	Maturity	Bioturbation	Skewness	Kurtosis	Notes
Mode	3 ÷ 2.5	0	Fine	0.8 ÷ 1.0	6	Imm÷PWsh	Very	+ 0.1	1.0	Fining-upward
SPANBOTH			3 ÷ 2.5				Common			grain size trend;
N = 10		Q up to	Coarse				up to			sorting regularly
Range	4 ÷ 2	1.3 mm	1.5 ÷ 1	0.6 ÷ 2.0	4 ÷ 9	Wck÷Sub	Intense	.3 ÷ -.3	0.8÷1.2	decreases upward
Mode	2.5÷1.5	1 ÷ -0.5	Fine	0.4 ÷ 0.8	5	PWsh÷SMat	Common	0	1.0	
DIBLING			3 ÷ 2.5							Coarsening-upward
N= 13		Q up to	Coarse				up to			cycles
Range	4 ÷ 1.5	2.2 mm	1.2 ÷ 1	0.3 ÷ 1.0	3 ÷ 8	Imm÷SMat	Intense	.2 ÷ -.2	0.8÷1.4	
Mode	2.2	0.5÷-0.5	Fine	0.5 ÷ 0.8	5	PWsh÷Sub	Minor	- 0.1	0.9	
STUMPATA			2.5							Coarsest samples
N= 12		Q up to	Coarse				up to			at the top
Range	2.5÷1.8	1.5 mm	1.6 ÷ 1.3	0.5 ÷ 0.9	4 ÷ 7	PWsh÷SMat	Intense	.2 ÷ -.2	0.9÷1.3	

Table 3 – Textural features of the Stumpata Quartzarenite in the Lower Zangla (Spanboth section, with 3 samples from Marpo), Upper Zangla (Dibling section, with 1 sample from Kanji) and Lingshed (Stumpata section) thrust sheets. Values of parameters are in Phi (ϕ) units. Skewness and kurtosis values are only indicative.

are very similar to those described by Goldbery (1979), with coarse sand–sized, subrounded and equant quartz dispersed in a ferruginous or micritic matrix. Quartz grains may display solution pits and opaque–filled microfractures.

Mineralogy. 3700 points were counted on 19 selected samples. All of them are quartz-arenites with more than 98% monocrystalline quartz grains (Fig. 6A), commonly showing tourmaline, zircon or apatite inclusions. Average main petrographic parameters are Q = 99,7, F = 0.1, L = 0.2 (after Dickinson, 1970; Q = Quartz; F = Feldspars; L = Lithics). Polycristalline to total quartz ratio (C/Q) is invariably under 3% and increases very slightly with grain size (correlation coefficient = 0.6, significant at the 5% level). Non quartzose detritus consists of rare felsitic lithic fragments or altered and untwinned feldspar grains, which tend to be smaller than quartz. Other types of rock fragments and microcline were never recorded. The ultrastable heavy mineral fraction, locally enriched in thin laminae, is characterized by subangular to perfectly rounded and spherical tourmaline grains (colourless, yellow, green, blu and zoned varieties; Fig. 6B), opaques, commonly abraded zircon and rutile. Micas and detrital matrix are lacking in non–burrowed sandstones. Intrabasinal grains are absent in most counted samples, but sporadic mud intraclasts, abundant and oversized bioclasts, phosphatized grains and peloids are found at the top of the unit (Fig. 6 C,D). Virtually all samples are cemented by syntaxial quartz, but in a few much mud (up to 27%) was introduced by burrowing activity. Primary cement ranges 0 to 14% in burrowed samples and 22 to 36% in weakly or non–bioturbated orthoquartzites, where interlocking overgrowths are generally 32 to 36%. For further details about sandstone petrography and adopted methodology see Garzanti (1986).

Faunal content and age.

The Stumpata Quartzarenite, which is comprised between the latest Maastrichtian *Siderolites* Beds and the Late Paleocene Dibling Limestone, does not contain age–diagnostic fossils. The Cretaceous/Tertiary boundary was placed by Gaetani et al. (1983) at the top of the sandstone unit, which at Spanboth yielded ostreids (*Odontogryphaea morgani* (Vredenburg)) and one crab (*Costacopluma concava* Collins & Morris) reported so far only from Upper Cretaceous strata. They concluded that the quartzarenites had been deposited during the

Fig. 5 – Stratigraphy of the Zanskar shelf across the Cretaceous/Tertiary boundary. The unconformities bracketing the Stumpata depositional sequence are dated, by correlation with Vail's coastal onlap curve and according to the geochronological scale of Berggren et al. (1985), at about 66 and 63 My. At this time (magnetic anomalies 29 to 27), the Zanskar shelf was about to cross the equator during the northward flight of peninsular India (Patriat & Achache, 1984). The unconformities at the base and top of the Stumpata Qzt. are probably of type 1 and 2 respectively, whereas the sharp base of the *Siderolites* Beds and top of the Main Qzt. body might be interpreted as type 3 paraconformities. These three kinds of hiatal surfaces are respectively ascribed to rapid eustatic fall, slow fall followed by rapid rise and decreased rate of relative sea–level rise (Vail & Todd, 1981). Only the upper part of the composite Marpo section was measured at Marpo; the main body of the unit was observed some km to the E, where its thickness tends to increase. (Si = silt; VFS & FS = very fine sand & fine sand).

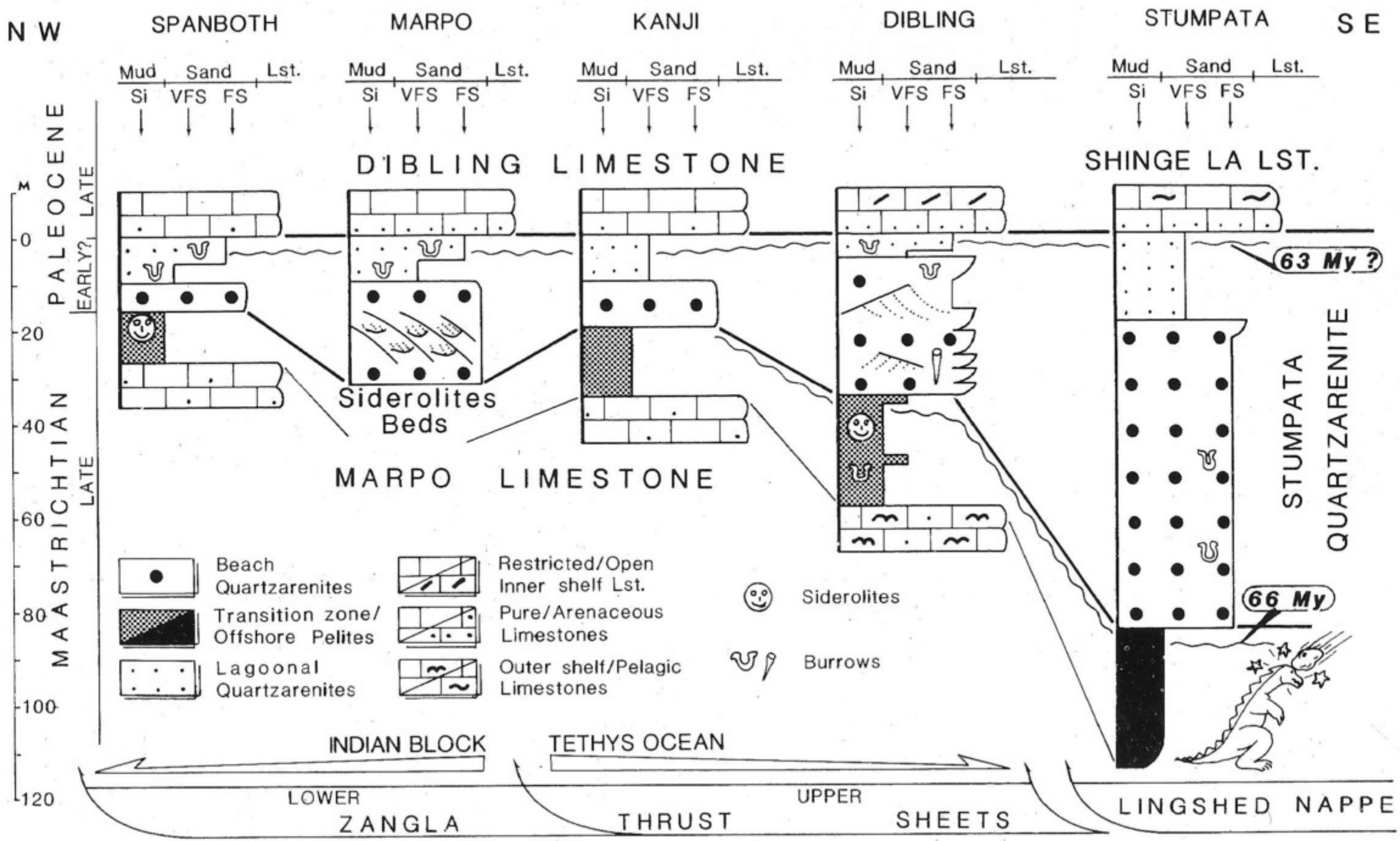
N W
S E
SPANBOTH
MARPO
KANJI
DIBLING
STUMPATA
Mud
Sand
Lst.
Si
VFS
FS
PALEOCENE
LATE
EARLY?
MAASTRICHTIAN
LATE
0
20
40
60
80
100
120
DIBLING LIMESTONE
SHINGE LA LST.
Siderolites Beds
MARPO LIMESTONE
STUMPATA QUARTZARENITE
63 My ?
66 My
Beach Quartzarenites
Transition zone/ Offshore Pelites
Lagoonal Quartzarenites
Restricted/Open Inner shelf Lst.
Pure/Arenaceous Limestones
Outer shelf/Pelagic Limestones
Siderolites
Burrows
INDIAN BLOCK
TETHYS OCEAN
LOWER
UPPER
ZANGLA
THRUST
SHEETS
LINGSHED NAPPE

STRATIGRAPHY & Environment	N°	Average Size Φ	Longest Axis Φ	Fine Coarse Size Φ Modes	Sorting $\sigma\Phi$	Maturity	BT	SK	KU	N°	MINERALOGY Q	CEM %	MAT %
CONDENS. INTERVAL Transgr. Shoreline	5	3 ÷ 2.5	0.5 ÷ -0.5	8 3 1.5	1 ÷ 2	Wck ÷ Imm	BT	+	0+	2	100	0	10 ÷ 40
UPPER QUARTZAREN. Washover?	5	3 ÷ 2.5	0 ÷ -0.5	3 1.5	0.8 ÷ 1	PWsh	BT	0+	+	3	100	0 ÷ 10	7 ÷ 23
Lagoon	2	4 ÷ 3.5	1.5	----	0.8	Imm ÷ PWsh	BT	0+	0+	2	≥ 99	3 ÷ 25	6 ÷ 27
MAIN QUARTZ. BODY Surf zone	15	2.5 ÷ 1.5	1 ÷ -1	2.5 1.5 ÷ 1	0.3 ÷ 0.8	Sub ÷ SMat	NO	-	-	9	≥ 99	23 ÷ 36	0 ÷ 1
Burrowed Shoreface	3	2.5 ÷ 2	0	2.5 1.5	0.8 ÷ 0.9	PWsh	BT	+	+	1	99	14	19
Non-burrowed Shoreface	2	2.5	1	----	0.4 ÷ 0.5	SMat	NO?	0-	0-	1	100	31	0
SIDEROLITES BEDS Lower Shoreface	3	4 ÷ 3	2	----	0.5 ÷ 0.8	PWsh	BT	+	0	1	99	11	16

Spanboth Marpo Dibl. Stum.

Table 4 – Sedimentography and stratigraphic distribution of textural features in the Stumpata Quartzarenite. The restricted average grain size ($1.5 \div 2.5\ \phi$) suggests that saltation was the dominant depositional mechanism in surf zone sandstones, whereas coarse sands primarily deposited by rolling and sliding are absent, as in most beaches of low–relief coastal plains. Lack of lower fine and finer sands, good sorting and common coarse skewed and platykurtic grain size distribution are also consistent with a beach environment, where grains up to about 140 μm tend to be kept in suspension by wave activity and carried offshore (Friedman, 1967). The coarse mode (tail) found in virtually all but very fine grained samples probably represents the rolling population (Visher, 1969). Very fine grained or fine skewed sands are found only close to fair–weather wave base or in low–energy lagoons, where partial mixing with interbedded immature sediments may occur due to burrowing activity. «Surf zone» samples may comprise some swash and overwash sands, all of which have very similar textural features (Stonecipher et al., 1984). Also burrowed shoreface and washover (?) sands cannot be distinguished petrographically. (BT = bioturbation; SK = skewness; KU = kurtosis; CEM = quartz cements; MAT = «matrix», comprising biologically introduced mud and authigenic interstitial phyllosilicates; recrystallized micrite in the topmost sample. N° = number of samples). Bars to the right show the sampled part of the four stratigraphic sections.

latest Maastrichtian, whereas most of the Danian was missing in the studied area. However, bed–by–bed correlation shows that the oyster– and crab–bearing beds at Spanboth are time–equivalent to layers yielding Paleocene foraminifera at Dibling (Fig. 7). The Cretaceous/Tertiary boundary thus lies at a lower level than previously stated, and most probably corresponds to the base of the Stumpata Quartzarenite. Conversely, the reported oysters and crab, kindred species of which are found in the Paleocene (Vredenburg, 1916; Collins & Morris, 1975), extend up into the Danian.

Sedimentary evolution.

The depositional model for the Stumpata sequence, based on a few

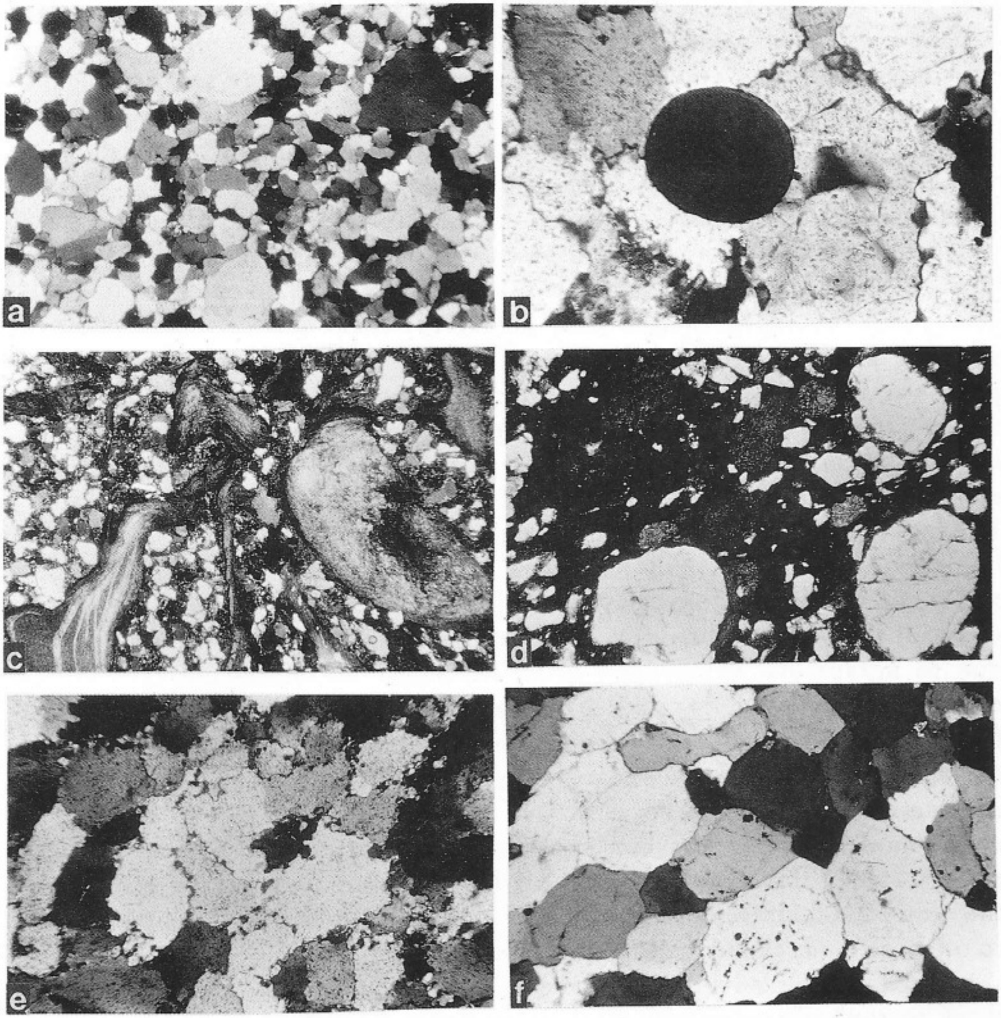

Fig. 6 – Sandstone petrofacies. a) Bimodally supermature surf zone orthoquartzite; Main Qzt. body at Stumpata (Q 54); x 20. b) Rounded and spherical blue tourmaline grain of likely polycyclic origin; Main Qzt. body at Spanboth (HZ 148); x 125. c) Poorly sorted bioclastic hybrid arenite rich in monospecific oysters; Upper Qzt. at Spanboth (HZ 152); x 13. d) Subrounded coarse sand–sized quartz grains with solution pits, set in a finer groundmass of very fine to fine grained subangular quartz and ferruginous matrix and peloids (cf. Goldbery, 1979, fig. 3). Textural inversion phenomena are ascribed to storm reworking during rapid transgression; condensed interval at Spanboth (HZ 152b); x 33. e) Migration and recrystallization of grain + cement boundaries in the anchimetamorphic Lower Zangla Nappe; Main Qzt. body at Spanboth (HZ 148); x 49. f) Latest Paleocene superstable and supermature quartz–cemented quartzarenite; note slight motion of crystal boundaries; Lithozone C of the Dibling Limestone, above Dibling (H 78); x 39.

measured sections and textural petrographical data, along with cursory observations at a limited number of other localities (Fig. 1), is here presented mainly to stimulate thinking and further detailed stratigraphical and sedimentological research. Lack of fossils and strong anchimetamorphic deformation hamper accurate correlation of the studied sections, which belong to three different thrust sheets (Gaetani et al., 1985b). Paleogeographical restoration is thus dependent on structural restoration also.

Sedimentological and paleontological evidence suggests a coastal depositional environment for the Stumpata Quartzarenite (Gaetani et al., 1980, 1983). The faunal content of the generally poorly exposed *Siderolites* Beds points to an open shallow–marine environment, and these low–energy sediments were probably deposited in a lower shoreface to transition zone setting. The commonly cross–bedded and bimodally supermature Stumpata quartzarenites are instead indicative of a high–energy beach environment, where continuous wave action effectively winnowed and sorted the sediment (Friedman, 1967, 1979). The lens–shaped Main qtz. body is interpreted as an aggrading mesotidal shoreline complex (Moslow, 1984; Reinson, 1984). Widespread bimodal grain size and roundness distributions may be ascribed to mixing by longshore currents of different first–cycle to multicycle detrital populations. Alternatively, it may be due to intrabasinal sedimentary processes, either co–movement of a mobile coarse fraction ($1.5 \div 1\ \phi$) with a finer fraction ($2.5\ \phi$) and/or mixing of shoreface and swash–overwash deposits owing to reworking by tidal currents or during storm or high wave–energy season (Taira & Scholle, 1979). The great thickness and lateral extension of surf zone sediments in the Stumpata area, where mud is lacking and bioturbation sporadic, are ascribed to strong wave activity (McCubbin, 1982; Winn et al., 1984). The Stumpata barrier island faced the nearly 2000 km wide Neotethys Ocean open to the NE, and passed laterally to offshore muds (Baud et al., in preparation).

Back–barrier environments might be widely represented in the Yelchang slices, tectonically overridden by the Lingshed Nappe (Baud et al., 1985; Gaetani et al., 1985b). The point bar–like sands found E of Marpo were possibly deposited in a meandering intertidal channel, passing laterally into interchannel lagoonal deposits (Fig. 3) (De Mowbray, 1983; Weimer et al., 1985, p. 102). The coarsening–upward cycles at Dibling are upward–shoaling sequences capped by cross–bedded sands probably deposited under tidal influence, and might record the progradation of a tidal delta, at the mouth of a tidal inlet. Tide–dominated shoreline complexes, in fact, characterize the mesotidal coasts of many modern passive margins facing wide oceans.

The Main quartzarenite body in the Zangla Nappe is overlain by burrowed, moderately sorted and fine grained sandstones, which possibly represent washover deposits interbedded with lagoonal sediments (Fig. 7). The arenaceous

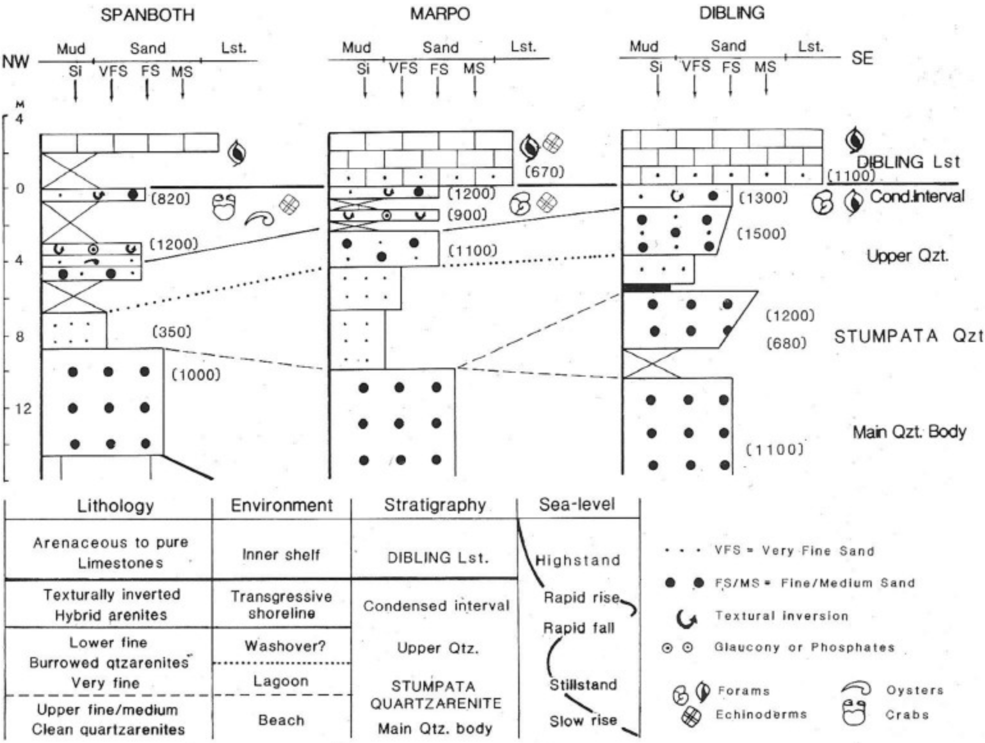

Fig. 7 – The transition between the Stumpata Quartzarenite and the Dibling Limestone is marked by a condensed interval related to landwàrd shift of terrigenous sedimentation during rapid transgression. Bed–by–bed correlation shows that layers at Spanboth, yielding oysters and crabs previously reported only in Upper Cretaceous strata, are equivalent to beds containing Tertiary foraminifera at Marpo and Dibling. The «Upper quartzarenites» in the inner Zanskar shelf can be subdivided into three stratigraphic intervals, which tend to coarsen oceanward (figures in brackets give maximum quartz grain diameter in microns), suggesting a backbarrier setting; coarser sands may have been deposited by washover processes. All Stumpata quartzarenites are calcite–free, but in the condensed interval carbonate abundance rapidly increases upward.

lenses yielding a monospecific oyster assemblage, found only in the most landward Spanboth section, point to brackish waters in transitional environments. The sedimentary evolution in the upper part of the Stumpata Qzt. thus seemingly shows a regressive trend with vertical transition to back–barrier facies, possibly related to a decreased rate of relative sea–level rise (Pitman, 1978). Next, the formation is capped by subrounded and muddy hybrid arenites. The occurrence of etched subrounded quartz grains set in a ferruginous groundmass indicates erosion of deeply–weathered coastal plain soils probably during shoreline retreat. Textural inversion phenomena suggest mixing of beach sediments with lagoonal pelites by storm and high wave activity (Goldbery, 1979).

These beds also contain «glaucony» and phosphate clasts and show a fining–upward sequence from poorly sorted sands to wackes with increasing carbonate content and open marine fossils. They are interpreted to represent a reworked lag deposited at the high–energy front of a transgression and to testify the drowning of the shoreline complex (Abbott, 1985). The Stumpata quartzarenites are overlain by a thin arenaceous limestone layer followed by pure high-stand carbonates.

Provenance.

The Zanskar Tethys Himalaya around the Cretaceous/Tertiary boundary was a wave–dominated coastal plain. Deposition was primarily controlled by eustatic fluctuations in an «interdeltaic» setting, with terrigenous detritus supplied by longshore transport from contemporaneous deltaic sources.

The ultrastable siliciclastics were ultimately derived from the Indian continental block, comprising Precambrian and Cambro–Ordovician megasutures (Gansser, 1964; Garzanti et al., 1986). Evidence for polycyclicity are the very low C/Q ratio even in medium grained sands, the occurrence of reworked overgrowths, the bimodal roundness of heavy minerals, the presence of perfectly rounded quartz and tourmaline grains, and the grain size bimodality (type 4 and type 5 textural inversion of Folk, 1980, p. 104) (Fig. 6 A,B). A few volcanic rock fragments and traces of chloritized biotite might represent the very scanty residual detritus derived from the active Deccan volcanics (Srivastava, 1983) and brought northward to the Tibetan passive margin during the latest Cretaceous . Slight volcanic input is in fact recorded also in the Kangi La Formation (Gaetani et al., 1983).

The exclusiveness of monocrystalline quartz grains in the Stumpata Quartzarenite is ascribed primarily to a wet subequatorial climate, favouring intense weathering in source rocks and coastal plains, and also to further maturation of partly polycyclic detritus in high–energy shoreline environments. In fact, paleomagnetic evidence shows that at this time the whole northern part of the Indian continent lay between 20° S and the equator (Klootwijk, 1979; Patriat & Achache, 1984; Savostin et al., 1986). This climatic interpretation is consistent with the occurrence of subrounded quartz grains showing solution pits, indicative of deep weathering (Cleary & Conolly, 1972).

On the origin of superstable passive margin quartzarenites.

Modern rivers draining highly weathered and low–relief cratonic blocks show a marked downstream increase in mineralogical stability, and transport to trailing–edge continental margins somewhat rounded sands which are often composed of more than 90% quartz (Cleary & Conolly, 1971; Potter, 1978, 1986; Johnsson et al., 1986). In subequatorial climates, therefore, passive margin quartzarenites can be produced in a single sedimentary cycle (Blatt, 1967; Folk, 1980, p. 139; Franzinelli & Potter, 1983; Suttner & Dutta, 1986). In many cases, however, appreciable amounts of feldspar grains are retained, and coarser beach quartzarenites pass laterally to fine and very fine sandstones deposited in adjacent lower–energy environments, which are mostly subarkoses and arkoses respectively (Odom, 1975; Odom et al., 1976; Mack, 1978; Garzanti, 1986). Exclusive monocrystalline quartzose detritus (Q = 100; C/Q = 0) in all grain size fractions and in all sedimentary environments testified in one depositional sequence represents a further, ultimate step towards mineralogical stability, and may require prominent multicyclic supply along with mechanical maturation in beach environments and/or extreme and prolonged chemical weathering in low –relief source areas to be attained (Suttner et al., 1981). Such a combination of factors is likely to be met in old passive margins lying close to the equator, as peninsular India around the Cretaceous/Tertiary boundary. These margins, bordering low–lying foreland blocks, would be characterized by low subsidence rates (typically 30 m/My; Schwab, 1976) and by well developed coastal plains mantled by deeply weathered soils, particularly since the appearance of flower plants in the mid–Cretaceous. Their coasts, facing wide oceans, are likely to be dominated by intense wave action and thus characterized by high–energy littoral sedimentation. Sandstone deposition, triggered by relative lowering of sea–level, would involve erosion and reworking of coastal terraces both during lowstand stages and due to shoreline retreat brought about by the subsequent transgression. Polymodal roundness, sphericity and grain size frequency distributions may be produced through mixing in various proportions by marine currents of first– and possibly also multi–cycle grains, yielded by major continental river deltas and derived from cratonic interiors and/or ancient megasutures, with policyclic detritus carried to the sea by shorter coastal plain streams (Mazzullo, 1986). Destruction of heavily altered unstable and semistable grains, if still present, is likely to proceed to completion in high–energy nearshore settings, owing to the low subsidence rate. Bimodally supermature pure quartzarenites would thus be typical products of fully–developed and subequatorial passive continental margins.

At this regard it may be worth noting that the Devonian Muth Quartzite, deposited in high–energy shoreline settings, has likewise attained this superstable stage (Gaetani et al., 1985a). The Muth Fm. is characterized by the same grain size bimodality (modes at about 1.5 and 2.5 ϕ), which is also found in Holocene sands from different coastal environments (river, beach, eolian) of the mature passive margins facing the Atlantic Ocean and the Gulf of Mexico (Taira & Scholle, 1979).

Dibling Limestone.

It is a new formation name here introduced for the about 200 m thick sequence well exposed at Dibling (Fig. 8). It is defined as the carbonate unit resting between the Stumpata Quartzarenite and the Chulung La Formation. It is thus equivalent to the upper part of Fuchs' Spanboth Formation and cor-

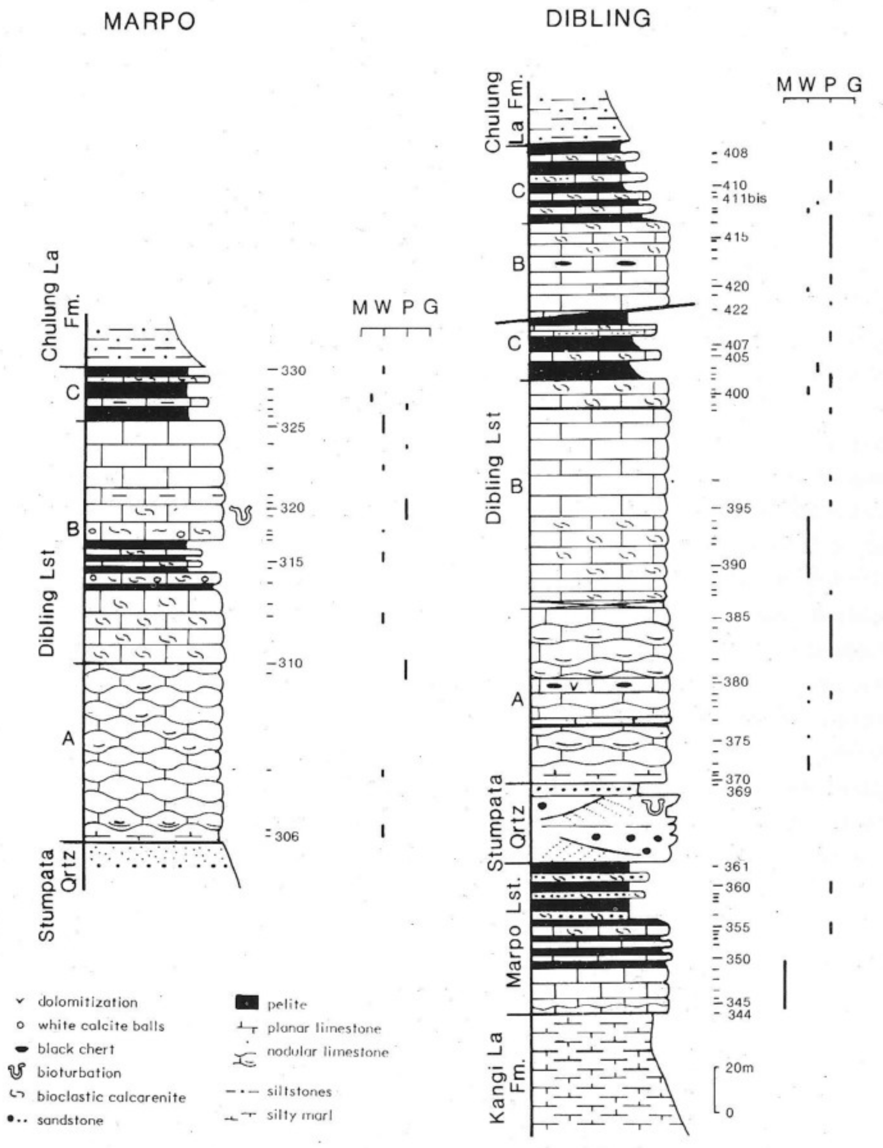

Fig. 8 – Marpo and Dibling sections with samples' location and distribution of microfacies (M = mudstone; W = wackestone; P = packstone; G = grainstone). Capital letters *A, B, C* refer to the lithozones of the Dibling Limestone.

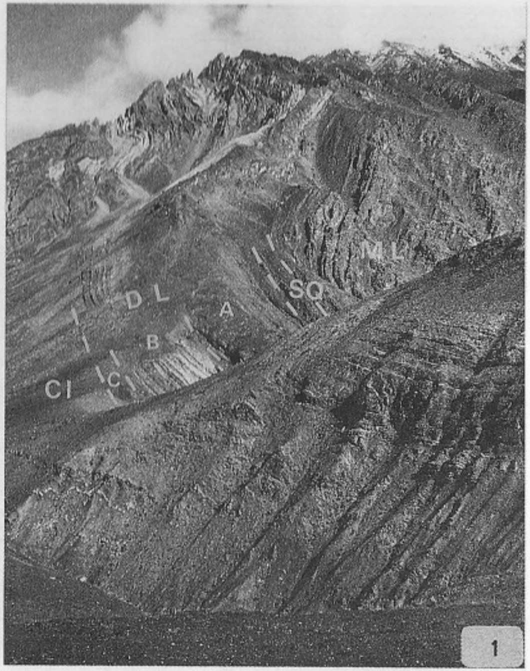

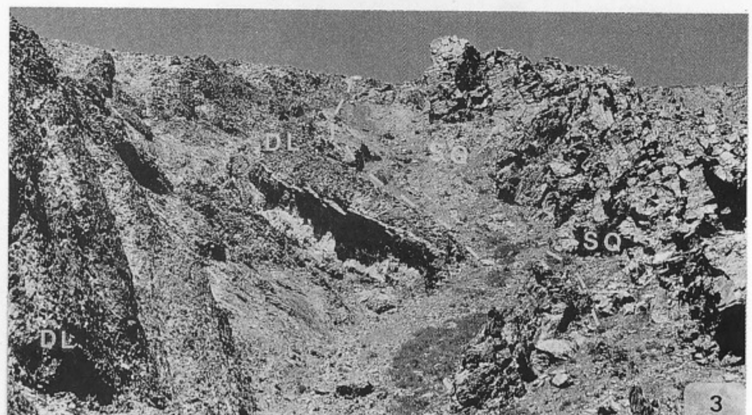

Fig. 9 – The Marpo section. 1) General view of the Cretaceous–Tertiary sequence (ML = Marpo Limestone; SQ = Stumpata Quartzarenite; DL = Dibling Limestone with lithozones *A*, *B*, *C*; Cl = Chulung La Formation). 2) Closer view with lithozones *A*, *B*, *C* of the Dibling Limestone. 3) The passage Stumpata Quartzarenite / Dibling Limestone. White dotted lines correspond to lithological boundaries.

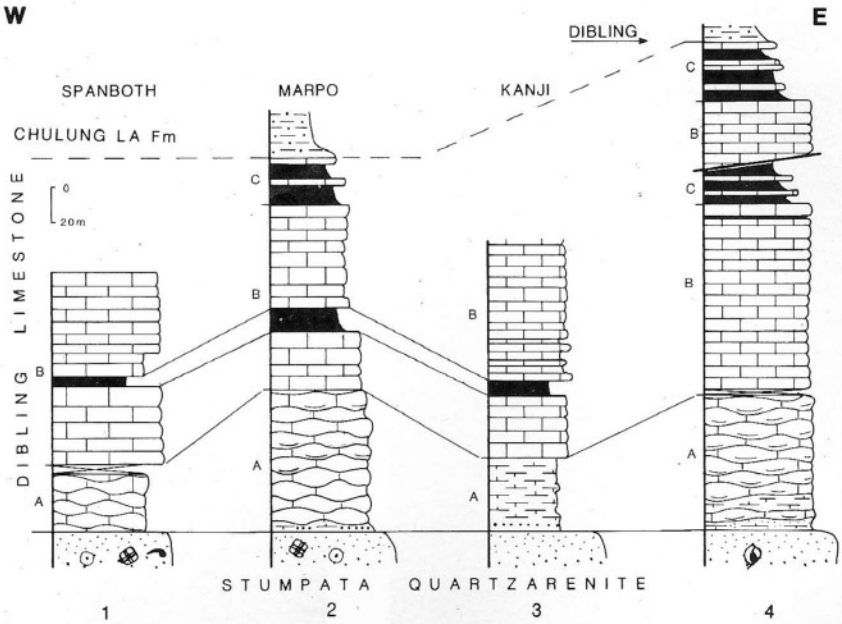

Fig. 10 — The Dibling Limestone and its lithozones *A, B, C* at Spanboth, Marpo, Kanji and Dibling. In the Dibling section, the upper part is tectonically repeated.

responds to the Upper or III° Member of the Spanboth Formation of Gaetani et al. (1983, 1985 a), Baud et al. (1984) and to levels 5 to 9 of Gaetani et al. (1980).

Its type–section is the one cropping out in the first gully NW of Dibling village where mills are located and it starts at 3990 m a.s.l.

Lithology.

The formation was studied at Marpo (Fig. 9) and Dibling, while partial sections in the lower/middle part were measured at Kanji and Spanboth (Gaetani et al., 1980, 1983). At Dibling, the upper part of the Dibling Limestone has been studied in two tectonically superposed slabs (Fig. 10).

In the type–area, the Dibling Limestone consists of three very distinctive lithozones (see Fig. 10 and fig. 16 in Gaetani et al., 1985a), from bottom to top:

Lithozone *A*: dark grey, nodular (Fig. 11), locally planar, bioclastic wackestones and subordinate (at Dibling) packstones with abundant micrite in 10–30 cm thick beds, generally amalgamated, interbedded with dark grey marls. Nodules mostly 5–15 cm in size, but smaller at the base of the unit, are bounded by thin yellowish weathered marly seams. Thick intercalations of grey marls are present at the base and also variously distributed within the lithozone especially at Dibling. At Marpo the pelitic fraction is less abundant, In the middle part, local dolomitization occurs and black chert nodules are present for about 4 m

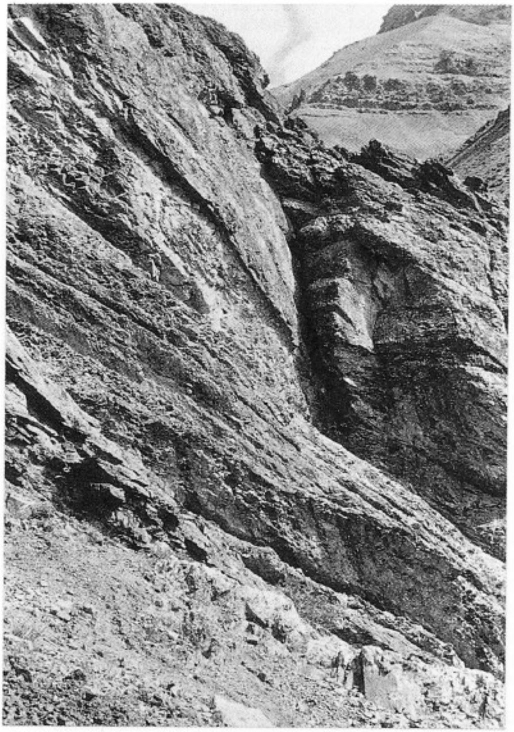

Fig. 11 – The topmost part of Lithozone *A*, Dibling Limestone, Dibling section.

Fig. 12 – Black chert nodules (10–20 cm) occur in the middle part of Lithozone *A*, Dibling Limestone, at Dibling.

(Dibling section, Fig. 12). The total thickness of Lithozone *A* is 79 m at Marpo and 76 m at Dibling, while it is reduced to only 30.6 m at Spanboth. It is replaced by some tens of meters of dark grey marly packstones at Kanji (Gaetani et al., 1980). With a sharp, generally covered passage.

Lithozone *B* follows: monotonous succession (about 110 m thick at Dibling) of bioturbated, planar, light grey, at the base, then dark grey, medium–bedded (10–30 cm thick) bioclastic packstones/wackestones alternating to fine bioclastic wackestones/packstones. Locally thick intercalations of dark marls and grey–greenish clays are present at Spanboth (5 m), Marpo (13 m) and Kanji (8 m in level 7 and marly horizons in level 9, Gaetani et al., 1980). The total thickness of Lithozone *B* varies from 105.7 m at Spanboth, to 101 m at Marpo. The nearly double thickness, about 200 m, of this lithozone at Kanji (Gaetani et al., 1980) is probably due to a tectonic repetition. At Spanboth and Kanji the upper part of Lithozone *B* is locally dolomitized. At Marpo, this unit is characterized by diffuse white calcite balls, larger (about 5 cm) at the base. Black chert nodules occur in the second tectonic slab of the Dibling section, in the lower part of the lithozone. Dark grey marls (30 cm at Marpo, 1.5 m at Dibling) mark the passage to the overlying.

Lithozone *C*: grey, greenish clays and marly clays (20–50 cm thick beds) with thin intercalations of planar to slightly nodular bioclastic calcarenites and calcareous siltstones with low–angle cross–lamination. The limestone intercalations show maximum thickness at the base (10–25 cm thick beds) while upwards only thin intercalations, 3–10 cm thick, are recorded. The clay fraction increases towards the top, where local enrichment of gastropods and other molluscs has been observed (Dibling section). Bioclastic wackestones prevail at Dibling, where silt–sized quartz extraclasts are found, whereas bioclastic packstones with subordinate wackestones and mudstones characterize the microfacies at Marpo.

Lithozone *C* has been studied only at Marpo (21 m thick) and Dibling (31 and 34 m thick) (Fig. 13). This lithozone is overlain by greenish rippled siltstones, still sporadically containing thin interlayered mudstones or wackestones and then by the Chulung La red beds.

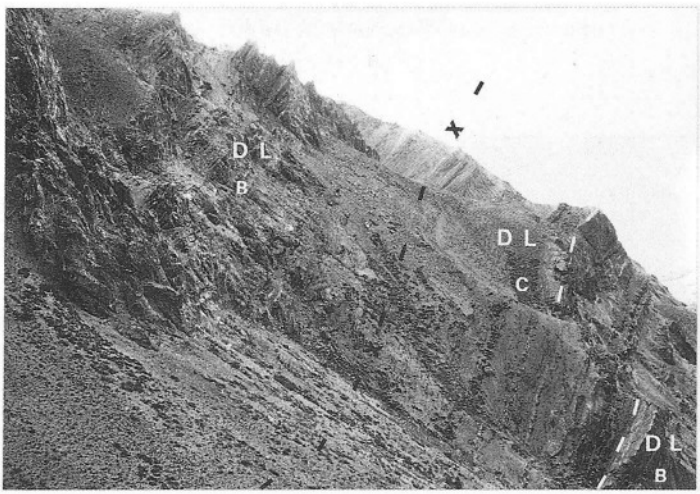

Fig. 13 – The upper part of Lithozone *B* and Lithozone *C*, Dibling Limestone, at Dibling. This photo shows the top of the lower slab (see Fig. 8, 10). White dotted line refers to lithological boundary. Black dotted line corresponds to the tectonic contact.
Higher up, in this section, other tectonic slabs occur with lithological sequences more similar to that of the Lingshed Nappe. In one of these, sandstone sample H 78 was collected.

Sandstone petrography.

The Dibling Limestone is mostly pure; sparse sand–sized quartz grains are found only in the basal layer immediately overlying the Stumpata Quartzarenite. However, a 8 m thick, cross–laminated sandstone lens showing lateral accretion bedding and scoured base was sampled in the lower part of Lithozone *C* in one of the highest tectonic slabs on the mountain above Dibling. The sample (H 78) is a medium grained (median diameter 340 μm; longest axis 2 mm), well sorted, coarse skewed, supermature quartzarenite cemented by syntaxial quartz overgrowths (Fig. 6F). Grain size distribution is slightly bimodal, with modes at about 210 and 430 μm. Subrounded monocrystalline quartz is exclusive ($Q = 100$; $C/Q = 0$). Small dolomite rhombs fill poorly developed intra–cement porosity.

Fossil content.

A rich fauna dominated by large rotaliids characterizes the Dibling Limestone where the following assemblage zones have been distinguished, from bottom to top:

Lockhartia–Rotalia Assemblage C.

Large rotaliids (*Lockhartia* sp., *L. heimei* (Davies), *Rotalia* sp., *R.* cf. *trochidiformis* Lamarck) associated with small foraminifera (*Marginulina* sp., *Dentalina* sp., *Gavelinella* sp., textulariids, *Chrysalidina*, miliolids), ostracods, crinoids, udoteacean Algae (*Ovulites* cf. *elongata* Lamarck, *O.* sp. aff. *kangpensis* Yu–Jing), dasycladacean Algae (*Furcoporella* cf. *diplopora* Pia, *F. diplopora* Pia, *Clypeina* cf. *merienda* Elliott (see also Assemblage H of Gaetani et al., 1983)) characterize the lower part of the Dibling Limestone (samples HZ 370–374, Dibling section; HZ 307, Marpo section). This assemblage strictly corresponds to Assemblage E of Gaetani et al. (1983), at Spanboth, while at Kanji, probably because of sparse sampling, it has not been observed.

Daviesina danieli Assemblage D.

Daviesina danieli Smout, rarer *D. khatiyahi* Smout, large rotaliids, *Operculina* sp., *Victoriellidae*, miliolids, *Ataxophragmiidae*, *Chrysalidina*, *Orbitolites* sp., bryozoans and ostracods represent this assemblage which is well developed in the Dibling section (samples HZ 375–377, about 20 m). The assemblage also contains dasycladacean Algae (*Clypeina* sp., *Trinocladus* sp.), corallinacean Algae (*Archaeolithothamnium* sp., *Distichoplax* sp., *Ethelia* sp. are especially developed at Kanji). This assemblage corresponds to Assemblage D (Gaetani et al., 1980) and only in part to Assemblage F of Gaetani et al. (1983).

Daviesina–Sphaerogypsina Assemblage E.

This association (samples HZ 378–383, Dibling section; HZ 308, 309, Marpo section) is characterized by abundant *Sphaerogypsina* sp., represented by both large and small forms. *Daviesina danieli* Smout is rare, but still present in the lowermost portion, while *D. khatiyahi* Smout becomes frequent. *D. langhami* Smout appears in the middle–upper part of the interval. In sample HZ 382 (Dibling section) a few specimens of *Fasciolites* (*Glomalveolina*) cf. *primaeva* (Reichel) firstly appear.

Ranikothalia sp., *Operculina* sp., *Orbitolites* sp., few large rotaliids, miliolids, *Ophthalmidiidae*, *Ataxophragmiidae*, bryozoans, rare corallinacean Algae remains (*Corallina* sp., *Jania* sp.) and few *Melobesiae* also characterize the assemblage. With respect to the Kanji and Spanboth sections, in the Marpo section and, particularly in the Dibling section, specimens of *Ranikothalia* are very abundant, well preserved and occur throughout the interval.

Daviesina langhami Assemblage F.

Daviesina langhami Smout, rarer *D. khatiyahi* Smout, *Ranikothalia* sp., *Operculina* sp., large miliolids, *Chrysalidina*, *Ataxophragmiidae*, *Orbitolites* sp.,

Formation	Lithozone	Samples not investigated	Samples investigated HZ	*Gavelinella sp.*	*Pseudochrysalidina sp.*	*Chrysalidina sp.*	*Lockhartia sp.*	*Rotalia sp.*	*Orbitolites sp.*	*Daviesina sp.*	*Daviesina danieli*	*Daviesina khatiyahi*	*Daviesina langhami*	*Operculina sp.*	*Ranikothalia sp.*	*Sphaerogypsina sp.*	*Fasciolites sp.*	*F. (G.) levis*	*F. (G.) subtilis*	*F. avellana*	*F. cucumiformis*	*F. ellipsoidalis*	*Textulariidae*	*Miliolidae*	*Ataxophragmiidae*	*Valvulinidae*	*Rotaliidae*	*Ovulites sp.*	*Ovulites cf. kangpensis*	*Furcoporella diplopora*	*Clypeina cf. merienda*	*Trinocladus sp.*	*Corallina sp.*	*Jania sp.*	Echinoids	Crinoids	Gastropods	Ostracods	Molluscs	Assemblages	Age
Dibling Limestone	C		330		O				X															●			O											O		L?	Late PALEOCENE
			329		●	O			X														O	●	●		O											O			
			328																																			O			
			327		●	O			X														O	O	O		O											O			
			326		O												X						X	O	X		O											X			
	B		325		O				X								O				?			O			O													I	
			324		●	O	X		X								●	O	●	O			O	O			O											O			
			323		O				?														O	O	O	O	O											X		H	
			322																								X											X			
			321		O	O			O									O	X				O	O	O		O														
			320		X												O	O						O	O		O											X			
			319		O	O		O									O	O					O	O	O	O	O											X			
		HZ 317	318																								O													G?	
			316																								X														
			315			O								X									X	X		O	O														
			314																					O													O	X			
			313			O																	O	O													O				
			312																																						
			311		O		O		O			O	O	O									O	O	X		O													F	
	A		310		O	O		X	O		X	O	O	X									X	O	O	O	O			O	O	O	X	X				O			
			309								X	O	X	O	X	O									X															E	
			308							O	O	O		O	X																									D	
			307	O	O	O	O	O															O		O		●	O	X	O	O				X		O	O	O	C	late Early
			306		O	O																	X	X	X	O	●	O		O	O				X				O		
			305																																						
			304		O		X																	O			O	●										X	X		
Stump. Quartz.			303																																		X				
			302																					X			X														
			301																					X			X														
			300																																						

Table 5 – Stratigraphic distribution and estimated abundance of the various fossil components in the Marpo section. ● = Very abundant, ○ = frequent, x = present.

rotaliids, briozoans, ostracods, scanty corallinacean Algae remains (Dibling section), dasycladacean Algae (*Clypeina* cf. *merienda* Elliott, *Furcoporella* cf. *diplopora* Pia, *Trinocladus* sp.) (Marpo section) characterize this assemblage which is well represented in all the studied sections. At Dibling, where the sampling was closest this assemblage develops for only 12 m (samples HZ 384–386) although well documented only in one sample (HZ 385), whereas at

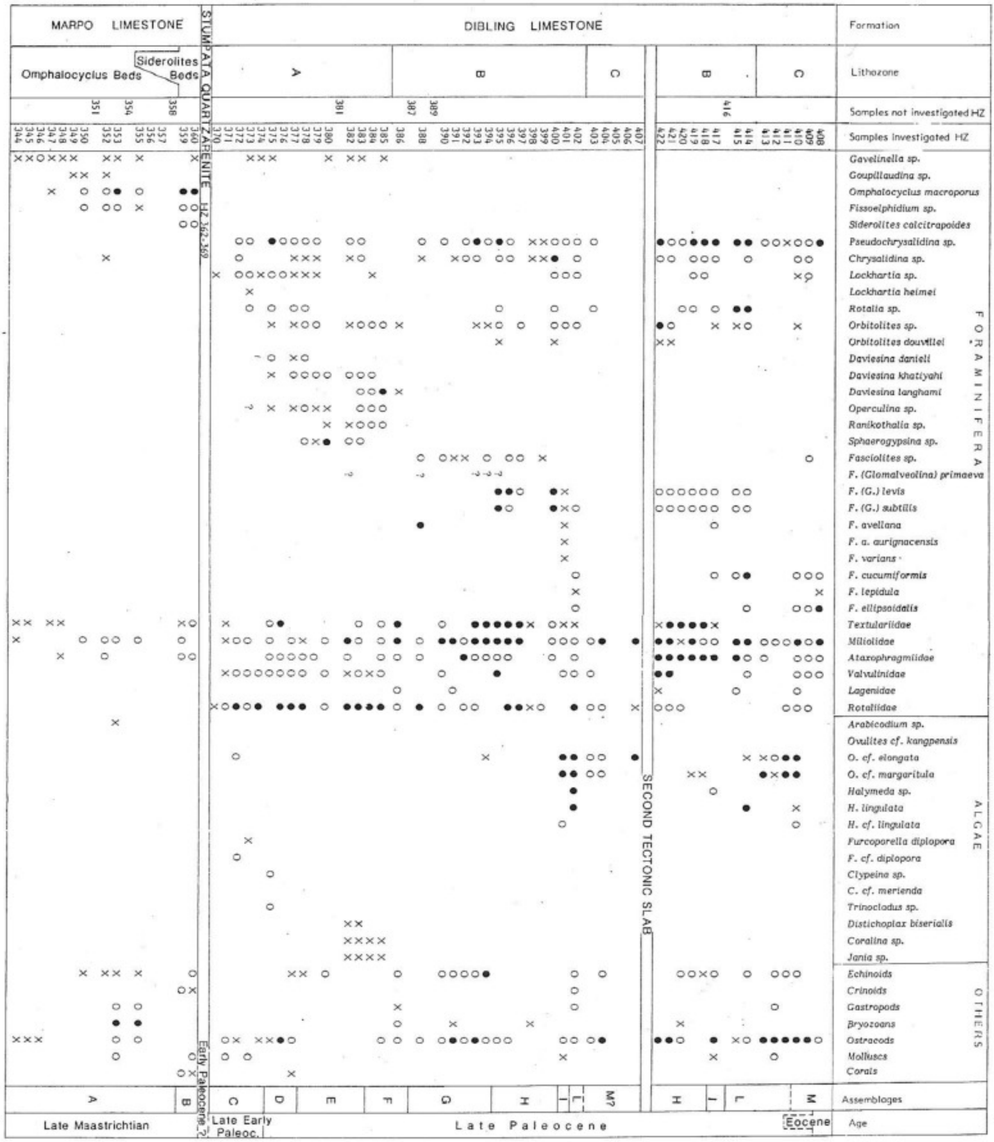

Table 6 – Stratigraphic distribution and estimated abundance of the various fossil components in the Dibling section. ● = Very abundant, ○ = frequent, x = present.

Marpo it ranges for at least 20 m (samples HZ 310–311) and at Spanboth it reaches about 35 m (samples HZ 179–185).

In the Kanji and Spanboth sections, the last samples collected contain this assemblage, as the uppermost portion of the Dibling Limestone was not investigated (Gaetani et al., 1980, 1983).

At Marpo and Dibling, where also the upper part has been investigated (Gaetani et al., 1985a) there is a very different fossil content above the *Daviesina langhami* Assemblage F, probably due to different paleogeographic condition. At Marpo, for more than 20 m (samples HZ 313–318) an association characterized by small, badly preserved foraminifera (miliolids, textulariids) and gastropods is present, while at Dibling representatives of the genus *Fasciolites* become frequent immediately above the *Daviesina langhami* Assemblage F, which develops in the upper portion of Lithozone *A* and at the base of Lithozone *B*.

In the higher part of the sequence, in both sections, the general trend of the fossil distribution is characterized by horizons with abundant and well preserved *Fasciolites* alternating to layers in which the fossil content is dominated by miliolids, textulariids, *Chrysalidina*, *Ataxophragmiidae*, while the genus *Fasciolites* is absent or represented by a few badly preserved specimens. The following assemblages have been identified.

Fasciolites (Glomalveolina) primaeva Assemblage G.

Fasciolites (Glomalveolina) cf. *primaeva* (Reichel) along with *Daviesina khatiyahi* Smout, *Orbitolites* sp., *Ranikothalia* sp., *Sphaerogypsina* sp., miliolids, textulariids, *Ataxophragmiidae, Chrysalidina*, echinoids was identified in sample HZ 382 (Dibling section, upper part of Lithozone *A*). Above this sample representatives of the genus *Fasciolites* are not present till sample HZ 388, where a few poorly preserved specimens were dubitatively attributed to *F. (G.) primaeva* (Reichel).

Higher up, the genus *Fasciolites* occurs up to sample HZ 394 with specimens highly deformed and badly preserved, while above, from sample HZ 395, the genus is represented by several well identifiable species. On these considerations we assume the interval between sample HZ 388 and HZ 394 as representing Hottinger's (1960 a, b) *primaeva* biozone. This zone in the Dibling section develops for about 28 m, in the Marpo section, it should correspond to the interval ranging from sample HZ 312 up to HZ 318 (37 m) where the fossil content is mostly represented by small foraminifera (miliolids, textulariids, *Chrysalidina*), while specimens of *Fasciolites* are not present.

Fasciolites (Glomalveolina) subtilis– F. (G.) levis Assemblage H.

The fauna of this assemblage is more diversified and well preserved than the previous one and consists of *F. (G.) subtilis* (Hottinger), *F. (G.) levis* (Hottinger), *Orbitolites* aff. *douvillei* (Nuttall), rotaliids, abundant *Chrysalidina, Ataxophragmiidae*, miliolids, textulariids associated with rare udoteacean Algae (*Ovulites* cf. *margaritula* (Lamarck), *O.* cf. *elongata* Lamarck). The assemblage is represented in samples HZ 395–400; 422–418 (tectonically repeated slab) at Dibling and HZ 319–321 at Marpo.

In the Marpo section, above Assemblage H, about 10 m (samples HZ 322, 323) are characterized by a microfauna consisting only of badly preserved foraminifera (miliolids, textulariids).

Fasciolites (Glomalveolina) subtilis–F. avellana Assemblage I.

F. (G.) subtilis (Hottinger), *F. avellana* (Hottinger), *F. avellana aurignacensis* (Hottinger), *F. cucumiformis* (Hottinger), *F.* cf. *varians* (Hottinger), *Orbitolites* sp., rotaliids, *Lockhartia* sp. occur in this association (samples HZ 401 and 417, Dibling section; HZ 324, 325, Marpo section) where also abundant udoteacean Algae (*Ovulites* cf. *elongata* Lamarck, *O.* cf. *margaritula* (Lamarck), *Halymeda* cf. *lingulata* Yu–Jing) are present.

Fasciolites cucumiformis Assemblage L.

Fasciolites cucumiformis (Hottinger), *F. (G.) subtilis* (Hottinger), *F.* cf. *ellipsoidalis* (Schwager), *Orbitolites* sp., rotaliids, *Lockhartia* sp., miliolids, *Ataxophragmiidae*, textulariids, very abundant udoteacean Algae (*Ovulites* cf. *margaritula* (Lamarck), *O.* cf. *elongata* Lamarck, *Halymeda lingulata* Yu–Jing) are the components. This assemblage characterizes the uppermost portion of Lithozone *B* (samples HZ 402 and 414, 415, Dibling section). The assemblage was not identified at Marpo.

The whole Lithozone *C* at Marpo (samples HZ 326–330) and its lower portion at Dibling (samples HZ 403–407; HZ 413–411) are characterized by abundant small foraminifera (textulariids, miliolids), large rotaliids, *Orbitolites* sp., very badly preserved *Fasciolites* and ostracods. Especially the Marpo fauna shows evidences of anchimetamorphic deformations.

Fasciolites ellipsoidalis Assemblage M.

In the tectonically repeated slab at Dibling, the last 16 m (samples HZ 410 –408) of the Dibling Limestone are dominated by a rich assemblage with *Fasciolites ellipsoidalis* (Schwager), *F. (G.)* aff. *subtilis* (Hottinger), *F. (G.)* aff. *lepidula* (Schwager), *Orbitolites* sp., rotaliids, *Lockhartia* sp., miliolids, ostracods, and abundant udoteacean Algae (*Ovulites margaritula* (Lamarck), *O.* cf. *elongata* Lamarck, *Halymeda lingulata* Yu–Jing).

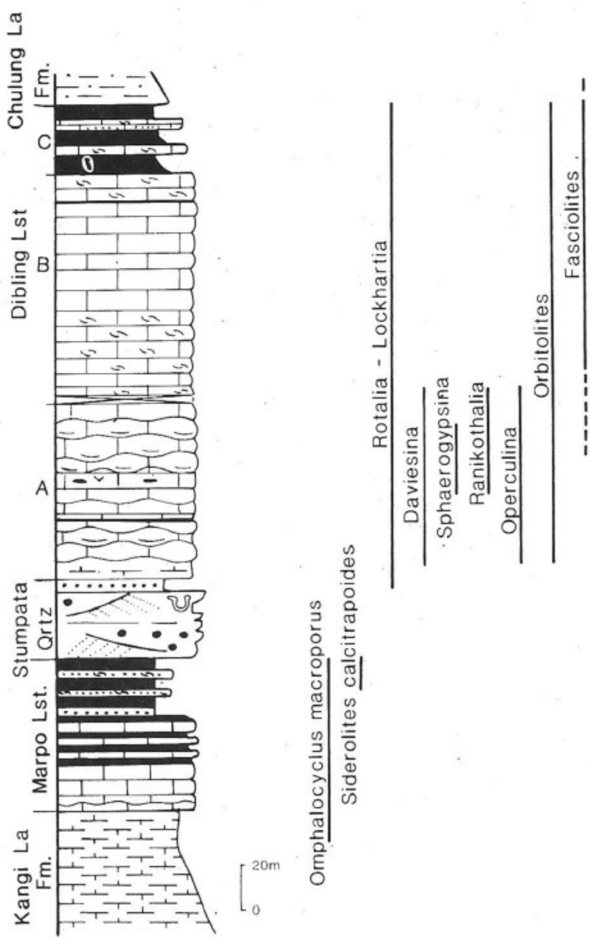

Fig. 14 – Distribution of the principal genera of benthic foraminifers in the Cretaceous–Tertiary sequence of Zanskar Range, Himalaya (Dibling section, summarized).

Age.

In the Dibling Limestone a unique, uninterrupted succession of benthic foraminiferal faunas occurs which can be syntetized in the following steps:

1) the base of the formation is characterized by large rotaliids (*Lockhartia* sp., *L. heimei* (Davies), *Rotalia* sp., *R.* cf. *trochidiformis* Lamarck). On this presence and on the absence of *Daviesina* a late Early Paleocene age (Smout, 1954; Nagappa, 1959) can be assumed for Assemblage C and consequently for the lowermost part of the Dibling Limestone;

2) the genus *Daviesina* in the Spanboth, Marpo and Dibling sections firstly appears about 2 m above the base of the formation. *Daviesina danieli* Smout,

which develops first and is supposed to be the ancestral form of the genus, begins shortly before *D. khatiyahi* Smout of Middle Paleocene age (Smout, 1954; Nagappa, 1959; Hasson, 1985). The last representative of the genus is *D. langhami* Smout which characterizes the upper part of Lithozone *A* and the lowermost portion of Lithozone *B* and indicates the Late Paleocene (Smout, 1954; Nagappa, 1959; Hasson, 1985). On these data Assemblages D, E, F, where the genus *Daviesina* is present in large amount, should indicate the Middle and Late (early) Paleocene (Smout, 1954; Nagappa, 1959; Hasson, 1985). Moreover, the presence of *Fasciolites (Glomalveolina)* cf. *primaeva* (Reichel) in sample HZ 382 (upper part of Assemblage E at Dibling) points to a Late (Thanetian) Paleocene age from the upper part of Lithozone *A*;

3) in Assemblages G, H, I, L and M where *Fasciolites* or *Fasciolites (Glomalveolina)* and *Orbitolites* are the most characteristic presences, a mostly continuous evolutionary sequence in the development of the genus *Fasciolites* has been noted. These assemblages perfectly correspond to the *primaeva, levis, cucumiformis* and *ellipsoidalis* biozones of Hottinger (1960 a, b). According to this author, Assemblages G, H, I are ascribed to the Thanetian p.p., while the *cucumiformis* (= Assemblage L) and the *ellipsoidalis* (= Assemblage M) represent the Early Ilerdian (Table 7).

Recently, new chronostratigraphic interpretations, mostly based on planktonic foraminifera and nannoplankton, have been proposed (Schaub, 1981; Berggren et al., 1984, 1985) (Table 7).

In Schaub (1981) the two following proposal are referred (Table 7):

1) the *primaeva* and *levis* biozones are Late Paleocene (Thanetian), at the base of the *cucumiformis* biozone the Paleocene/Eocene boundary occurs, the *cucumiformis* and *ellipsoidalis* biozones represent the Early Ilerdian;

2) the *primaeva* and *levis* biozones are Middle Paleocene, the Paleocene/Eocene boundary is at the base of the *oblonga* biozone, the *cucumiformis* and *ellipsoidalis* biozones represent the lower part of the Late Paleocene.

In Berggren et al. (1984, 1985), the Late Paleocene is represented by the Thanetian (middle/upper P4, P5, P6a–planktonic zones), while the Early Eocene is represented by the Ypresian. The Paleocene/Eocene boundary corresponds to the boundary *Discoaster multiradiatus/Marthastarites contortus* nannoplankton biozones or *Morozovella velascoensis/M. edgari* (P6a/P6b–planktonic foraminifera), which means that it falls in the *ellipsoidalis* biozone.

Following Berggren et al. (1984, 1985), the present Assemblages G, H, I belong to Plankton Zone P4, Assemblage L falls in P5 while Assemblage M in P6. According to these data, the Dibling Limestone spans a time ranging from late Early Paleocene to the latest Paleocene. The Eocene/Paleocene boundary can be supposed in its topmost part.

BERGGREN et al., 1984 ; 1985

Chron	Planktonic forams			Age		Nannoplancton	
C24	P8		*Morozovella aragonensis*	Early EOCENE	Ypresian	NP12	*Marthasterites tribrachiatus*
C24	P7		*Morozovella formosa formosa*	Early EOCENE	Ypresian	NP11	*Discoaster binodosus*
C24	P6	b	*Morozovella subbotinae*	Early EOCENE	Ypresian	NP11	*Discoaster binodosus*
C24	P6	b	*Morozovella edgari*	Early EOCENE	Ypresian	NP10	*Marthasterites contortus*
C24	P6	a	*Morozovella velascoensis*	Late PALEOCENE	Selandian Thanethian	NP9	*Discoaster multiradiatus*
C25	P5		*Morozovella velascoensis*	Late PALEOCENE	Selandian Thanethian	NP9	*Discoaster multiradiatus*
C25	P4		*Planorotalites pseudomenardi*	Late PALEOCENE	Selandian Thanethian	NP8	*Hel. riedeli*
C25	P4		*Planorotalites pseudomenardi*	Late PALEOCENE	Selandian Thanethian	NP7	*Disc. gemmeus*
C26	P3	b	*Planorotalites pusilla pusilla*	Late PALEOCENE	Selandian unnamed	NP6	*Hel. kleinpelli*
C26	P3	b	*Planorotalites pusilla pusilla*	Late PALEOCENE	Selandian unnamed	NP5	*Fasciculithus tympaniformis*
C26	P3	a	*M. angulata*	Early PALEOCENE	Danian	NP5	*Fasciculithus tympaniformis*
C26	P2		*Morozovella uncinata*	Early PALEOCENE	Danian	NP4	*Ellipsolithus macellus*
C27	P1	c	*Subbotina trinididadensis*	Early PALEOCENE	Danian	NP3	*Chiasm. danicus*
C28	P1	b	*Subbotina pseudobulloides*	Early PALEOCENE	Danian	NP2	*Crucipl. tenuis*
C29	P1	a	*"Glabigerinita" eugubina*	Early PALEOCENE	Danian	NP1	*Markal.inversus*
C29			*Abathomphalus mayaroensis*	Late Cretaceous	Maastric		
C30			*Abathomphalus mayaroensis*	Late Cretaceous	Maastric		

SCHAUB, 1981

Alveolina		Age	
oblonga	EOCENE	Cuisian (2)	Upper
trempina	EOCENE	Ilerdian	Middle
corbarica	EOCENE	Ilerdian	Middle
moussolensis	EOCENE	Ilerdian	Middle
ellipsoidalis	EOCENE	Ilerdian	Lower
cucumiformis	EOCENE	Ilerdian (1)	Lower
levis	PALEOCENE	Thanetian	Upper
primaeva	PALEOCENE	Thanetian	Lower
	PALEOCENE	Danian	

HOTTINGER, 1960 a; b

Alveolina	Age		
oblonga	Cuisian	Lower	EOCENE
trempina	Ilerdian	Upper	EOCENE
corbarica	Ilerdian	Middle	EOCENE
moussolensis	Ilerdian	Middle	EOCENE
ellipsoidalis	Ilerdian	Lower	EOCENE
cucumiformis	Ilerdian	Lower	EOCENE
levis	Thanetiano p.p.	Montian p.p.	PALEOCENE
primaeva	Thanetiano p.p.	Montian p.p.	PALEOCENE
	Danian		PALEOCENE

Table 7 – Table of biostratigraphic and chronologic correlations: a) Paleocene time–scale according to Berggren et al., 1984, 1985; b) Late Cretaceous–Early Eocene biozones and position of the Paleocene–Eocene boundary (1) between Thanetian and Ilerdian, (2) between Ilerdian and Cuisian (Schaub, 1981); c) Biozones and ages according to Hottinger, 1960 a, b.

Sedimentary evolution.

The Dibling Limestone was deposited on an inner carbonate shelf, evolving from open (Lithozone *A*) to protected conditions (Lithozones *B* and *C*). The unit thus records an overall regressive trend from the initial sharp deepening event at the top of the Stumpata Quartzarenite to the lagoonal facies of Lithozone *C*. The more varied fossil assemblages of Lithozone *A*, consisting of widespread nodular bioturbated bioclastic wackestones with subordinate packstones and marly intercalations, are indicative of an open shelf, only episodically affected by waves or tidal currents. The more abundant pelitic intervals at Dibling with respect to the Marpo and Spanboth areas suggest the lateral transition to a more distal and undisturbed environment toward the east.

The rapid vertical transition to Lithozone *B*, which consists of planar bioclastic packstones to often bioturbated wackestones with more and more abundant alveolinids and miliolids, indicating more restricted conditions, is ascribed to outward facies migration. This regressive event, occurring during zone P4, is possibly related to a decreased rate of relative sea–level rise (Pitman, 1978). Lithozone *C*, consisting of marls with minor intercalations of bioclastic calcarenites and cross–laminated siltstones, and containing a fauna and flora dominated by porcelaneous benthic forams and udoteacean Algae, testifies to an even more restricted depositional environment, with widespread fine grained terrigenous detritus deposited under the action of weak meteorological currents.

Depositional history: sedimentation and sea level changes.

The Marpo Limestone represents a shallow–water carbonate ramp with depositional environment gradually deepening from inner infralittoral in the SW (Lower Zangla Nappe) to circalittoral in the NE (Upper Zangla Nappe) and finally passing to outer shelf/slope offshore pelites (Lingshed Nappe). The occurrence of common silt–sized quartz in the upper part of the *Omphalocyclus* Beds and of lower very fine grained sandstones in the *Siderolites* Beds indicates an increasing terrigenous pollution, due to a progressive eustatic lowering of base–level at the top of the Maastrichtian. Next, the sharp base of the Stumpata Quartzarenite represents a basinward shift of coastal onlap marked by the abrupt superposition of shoreline sands on top of transition zone (Zangla thrust sheets) to offshore sediments (Lingshed Nappe).

This unconformable contact was caused by erosion and reworking of shelf deposits while the shoreline was moving towards the shelfbreak during sea–level fall (Pitman & Golovchenko, 1983). Greater thermal subsidence close to the shelf edge and differential compaction of the underlying Late Cretaceous offshore muds cannot wholly account for the much greater thickness of the quartzarenites in the Lingshed Nappe, which indicates progressive SW–ward coastal onlap. Correlation with the global eustatic curve suggests that the Stumpata quartzarenites gradually onlapped the underlying top–Cretaceous unconformity during the Early Paleocene relative sea–level rise (Vail et al., 1977). The phosphate– and glaucony–bearing condensed interval (Fig. 7) found at the top of the Stumpata Quartzarenite attests to sediment starvation during rapid transgression, possibly following the mid–Paleocene global lowstand (Vail et al., 1977). If both this interpretation and the geochronological calibrations of Berggren et al. (1985) are correct, the Stumpata depositional sequence was deposited from 66 My to about 63 My, with average sedimentation rates increasing towards the shelf edge from 5 m/My at Spanboth to 30 m/My at Stumpata (Fig. 5).

In the Late Paleocene, the inner shelf Dibling Limestone in the Zangla thrust sheets and the deeper–water Shinge La Limestone in the Lingshed Nappe testify to highstand sedimentation without terrigenous pollution. Water depth returned in all stratigraphic sections equal or slightly less than in the latest Cretaceous, after the regressive Stumpata event (Fig. 5). The sea–bottom still sloped down towards the NE, passing from neritic conditions in the Zangla thrust sheets to upper bathyal environments in the Lingshed Nappe. Sedimentation was directly controlled by eustatic fluctuations, tectonic components other than steady thermal subsidence being negligible.

According to the geochronological scale of Berggren et al. (1985), the Dibling Limestone was deposited within about 5 My (from about 62 to 57 My). Lithozones *A* (about 75 m thick, planktonic zones P2 to P4) and *B* (about 100 m thick, zones P4 to P5) may roughly represent a time–span of 2 My each, whereas Lithozone *C* (20 to 30 m thick, zone P6) was probably deposited in less than 1 My. Average sedimentation rates on the inner part of the Zanskar shelf during the Late Paleocene were 35 to 40 m/My, which are comparable with those of the Late Cretaceous Kangi La Fm. (Baud et al., 1984).

On eustatic unconformities and formation boundaries.

The final regression at the close of the Cretaceous, heralded by a few tens of metres of silty carbonates at the top of the Marpo Limestone, is marked by the rapid transition from marls with interbedded very fine grained or calcareous sandstones to clean orthoquartzites. During rapid transgression at the top of the Stumpata Qzt., instead, non–calcareous quartzarenites pass upward to hybrid arenites, shortly followed by arenaceous limestones and then by pure highstand carbonates. Periods of rapidly changing sea–level and condensed sedimentation favoured the early diagenesis and induration of the sea–bed in presence of fresh to marine waters, with authigenic growth of microcrystalline quartz, phosphates and glaucony. Lithology, diagenesis and grain size of siliciclastic detritus are thus directly controlled by eustatic fluctuations of base–level.

Sandstone/carbonate transitions are rapid but gradual, and they occur within a few metres at most (Fig. 7). The precise location of unconformities is not always obvious in the field, particularly when their subtle geometry is dimmed by tectonic deformation. Biostratigraphic evidence suggests that major gaps most likely occur within the upper part of the finer grained arenitic intervals overlying and underlying the Stumpata Main quartzarenite body (Fig. 5). Depositional sequence and formation boundaries may thus not exactly correspond. In fact, whereas unconformities (depositional sequence boundaries) developed during maximum rate of sea–level fall (Vail et al., 1984), the appearance of pure Stumpata quartzarenites and of pure Dibling limestones (formation boundaries) seems to be related to the attainment of lowstand and highstand conditions respectively. Whilst the Marpo and Dibling limestones are composite lithostratigraphic units deposited during more than one third–order sea–level cycle, most of the Stumpata Quartzarenite may represent a single depositional sequence.

The end of passive margin sedimentation.

The cross–bedded sandstone body found in the upper part of the Dibling Limestone (base of Lithozone *C* high above Dibling) was probably deposited in a channel incised during an abrupt relative sea–level fall very close to the Paleocene/Eocene boundary. This erosive event does not correspond to a major «sawtooth» on Vail's curve and it probably has a mostly tectonic nature, related to the very onset of the India–Eurasia collision.

Paleomagnetic data from the Indian Ocean floor (Patriat & Achache, 1984), calibrated with the geochronological scale of Berggren et al. (1985), indicate that the Zanskar margin at the end of the Paleocene had already crossed the equator, and lay about 5°N, no more than 500 ÷ 600 km away from Asia. It is thus possible that at this time the subduction complex of the Transhimalaya arc–trench system had already begun to override the toe of the Indian continental rise (Lamayuru Unit), causing initial bulging of the continental terrace (Speed & Sleep, 1982; Stockmal et al., 1986; step II in fig. 2). The occurrence of latest Paleocene supermature and superstable sandstones ultimately derived from the craton interiors of the Indian continental block (Dickinson & Suczek, 1979), attests that detritus from the arc–trench systems bordering the northern Eurasian plate did not reach the trailing–edge margin of peninsular India until the Early Eocene (Gaetani et al., 1985 a).

The end of passive margin sedimentation, with passage to the Chulung La foreland basin volcanic arenites (Garzanti et al., in preparation), cannot be dated directly, for these fluvio–deltaic redbeds lack fossils. However, if the influx of volcaniclastic detritus shed from the uplifted Asian active margin is considered to be an isochronous event, the Chulung La Fm. of the Zangla Nappe would be time–correlative with the shallow–marine Kong volcanic siltstones of the Lingshed Nappe (Fuchs, 1982, 1986), which are mid–Early Eocene in age (P8 zone; Baud et al., in preparation). If so, the boundary between the Dibling Limestone and the Chulung La Formation in the inner part of the Indian continental margin would correspond to a disconformity with an associated erosional hiatus of about 3 My. The unconformity would pass seaward to shallow–water nummulitic limestones, deposited during Early Eocene zones P6 to P8 (Kesi Fm. of the Lingshed Nappe; Baud et al., in preparation). This downward shift of coastal onlap, marking the final closure of the Neotethys Ocean in Ladakh, is slightly older than the major pre–Middle Eocene global sea–level fall of Vail et al. (1977).

Burial history: from shallow diagenesis to orogenic metamorphism.

The latest Cretaceous to Paleogene succession of the Zanskar shelf passed rapidly from semi–mature diagenetic stage (Schmidt & McDonald, 1979), during the last million years of passive margin sedimentation, to supermature stage during the Himalayan orogeny. The high minus–cement porosity of the moderately well sorted Paleocene quartzarenites indicates that pores were occluded chemically in the early stages of diagenesis, before significant compaction. Quartz cementation by subvertically circulating groundwaters (Blatt, 1979; Dutta & Suttner, 1986) was completed rapidly (within 10–20 My) and at shallow depths (a few hundred metres), prior to continental collision.

During the Himalayan tectonic event, plastic deformation of quartz grains and cements or calcite was widespread. These processes were most intense in the Lower Zangla thrust sheet, where carbonate units are strongly recrystallized and quartzarenites show quartz sub–grains up to 20 μm in size, newly formed predominantly on the rims of strained overgrown detrital grains (Fig. 6E). Polygonization with intragranular recrystallization led to the formation of common pseudo–polycristalline quartz at Spanboth. In finer–grained sandstones, sub–grain development was hindered by the occurrence of interstitial phyllosilicates and quartz is much less deformed («cushioning effect» of Siever, 1959). Phyllosilicates are recrystallized to chlorite and hydromica beards, which reach 40 μm in length and peripherally replace siliciclasts. At the top of the Stumpata Qtz., brown pleochroic micaceous aggregates, which are most probably stilpnomelane, grew at the expense of glaucony peloids (Spanboth, sample HZ 152b), while zoisite seemingly formed at Marpo (HZ 301). Zoisite is still recorded at Marpo in the Chulung La redbeds, along with common authigenic epidote.

In the Marpo and Dibling Limestones of the Upper Zangla Nappe, fossils are better preserved due to less extensive calcite recrystallization (confront paleontologic plates in Gaetani et al., 1980 and 1983). Quartz deformation is also less prominent both in the Upper Zangla (Dibling, Kanji) and Lingshed Nappes, where quartz grains and cements still display undulose to segmented extinction and deformation lamellae, but without formation of newly–grown crystals (Fig. 6 A, F), Clinozoisite and pistacite are found in the volcanic arenites capping the Zanskar sequence at Dibling.

During the Himalayan event, the Lower and Upper Zangla Nappes were deformed at different metamorphic conditions. In the Lower Zangla Nappe, deformational features of quartz («zone of quartzitic structures»; Kossovskaya & Shutov, 1970) and the likely occurrence of stilpnomelane point to upper anchizonal conditions comparable to prehnite–pumpellyite metamorphic facies, at temperatures probably exceeding 300°C (Frey, 1970; Frey et al., 1973). In the less deeply buried Upper Zangla Nappe, only incipient migration of grain boundaries in Paleocene quartzarenites testifies to somewhat lower temperatures, around 275°C (Voll, 1982). Anchimetamorphic temperatures exceeding at least 220°–250°C (Cavarretta et al., 1984; Schifmann et al., 1984) and decreasing upward within the pile of nappes are testified also by the widespread occurrence of authigenic epidote in the Eocene Chulung La Formation, at the top of the Tethys Himalaya succession.

Conclusions.

The Zanskar passive margin records an overall shallowing–upward trend around the Cretaceous/Tertiary boundary (Fuchs, 1979; Baud et al., 1984). Lowering of sea–level at a rate higher than subsidence causes at first terrigenous pollution of the Marpo carbonate ramp (*Siderolites* Beds) and then migration of the shoreline toward the shelf edge, with exposure and erosion of a large part of the continental shelf at the close of the Cretaceous. Next, the rate of sea–level fall decreases and coastal encroachement ensues due to continuing thermal subsidence. The coastal Stumpata quartzarenites onlap the underlying unconformity and point to balanced terrigenous yield during slow relative sea–level rise in the Early Paleocene. At the top of the formation, finer– grained and burrowed regressive sandstones are followed by a condensed interval, indicating rapid eustatic transgression close to the Early/Late Paleocene boundary. In the Late Paleocene, widespread pure carbonates testify to highstand conditions without siliciclastic influx. The Dibling Limestone records an overall regressive trend from open to restricted inner shelf environments, as testified by the occurrence of progressively less diversified fauna and flora assemblages.

The Maastrichtian to Paleocene western Zanskar sequence was deposited on a NE–ward sloping passive margin continental shelf, prior to flexural bending towards the northern subduction zone. Average sedimentation rates during deposition of Late Cretaceous to Late Paleocene highstand carbonate units were around 35 ÷ 40 m/My. During deposition of the Stumpata Quartzarenite, owing to low sea–level and hiata development related to rapid eustatic fluctuations, average rates dropped to only a few m/My close to the hinge line, gradually increasing toward the shelfbreak up to a maximum of 30 m/My. Until the end of the Paleocene, siliciclastic detritus was exclusively supplied to the Zanskar shelf by sub–equatorial rivers draining the low–relief and deeply weathered southern Indian craton and coastal plains. Only in the Early Eocene did detritus from the north, shed from the obducting Eurasian accretionary prism, reach the Zanskar continental shelf. The petrography of the Chulung La redbeds thus testifies to the final closure of the Neotethys Ocean in Ladakh and to the formation of a proto–Himalayan mountain chain (Garzanti et al., in preparation).

The rapid transition from passive margin to overthrust belt is also recorded by the burial history of the Tertiary stratigraphic sequence, passing directly from shallow diagenesis prior to continental collision to very low grade metamorphic conditions under a tectonic load of nearly 10 km, as a result of foreland–directed thrusting and nappe stacking during the Himalayan orogeny.

Acknowledgments.

Many thanks to Maurizio Gaetani and Isabella Premoli Silva for encouragement and discussion, and to Carla Rossi Ronchetti for critical revision of the manuscript. We are grateful to Franco Fonnesu (AGIP, Milano), Mario Gnaccolini and Mario Fornaciari (Milano), Ruth Haas and Eveline Herren (ETH, Zürich) and to Gian Gabriele Ori (Bologna) for helpful criticism. Flavio Jadoul measured with us the Dibling section.

REFERENCES

Abbot W.O. (1985) - The recognition and mapping of a basal transgressive sand from outcrop, subsurface and seismic data. *Am. Ass. Petr. Geol., Mem.* n. 39, pp. 157–167, Tulsa.

Bassoullet J.P., Bernier P., Deloffre R., Genot P., Poncet J. & Roux A. (1983) - Les Algues Udoteacées du Paléozoique au Cénozoique. *Bull. Centr. Rech. Explor. Prod. Elf–Aquitaine*, v. 7, n. 2, pp. 449–621, 16 pl., 16 tab., 13 fig., Pau.

Bassoullet J.P., Colchen M., Juteau Th., Marcoux J., Mascle G. & Reibel G. (1983) - Geological studies in the Indus suture zone of Ladakh (Himalayas). In Gupta V.J. (Ed.) - Stratigraphy and structure of Kashmir and Ladakh Himalaya. Contributions to Himalayan geology, v. 2, pp. 96–124, Hindustani, Delhi.

Baud A., Gaetani M., Garzanti E., Fois E., Nicora A. & Tintori A. (1984) - Geological observations in southeastern Zanskar and adjacent Lahul area (northwestern Himalaya). *Ecl. Geol. Helv.*, v. 77, n. 1, pp. 171–197, Basel.

Baud A., Garzanti E. & Mascle G. (1985) - Latest marine sediments (Early Paleogene), geological events and nappe structure in central Zanskar area (NW Himalaya). Himalayan workshop abstracts, Leicester.

Baud A., Garzanti E. & Mascle G. (in preparation) - Latest marine sediments of the Zanskar outer shelf, Ladakh, India.

Berggren W.A., Kent D.V. & Flynn J.J. (1984) - Paleogene Geochronology and Chronostratigraphy. In Snelling N.J. (Ed.) - Geochronology and the Geologic Time Scale. *Geol. Soc. London, Sp. Pap.*, 138 pp., 4 appendix, 6 fig. (Preprint: Woods Hole Oceanographic Institution) Woods Hole, Massachussetts.

Berggren W.A., Kent D.V., Flynn J.J. & Van Couvering J.A. (1985) - Cenozoic geochronology. *Geol. Soc. Am. Bull.*, v. 96, n. 11, pp. 1407–1418, 6 fig., 3 tab., Boulder, Colorado.

Blatt H. (1967) - Provenance determinations and recycling of sediments. *Journ. Sedim. Petr.*, v. 37, pp. 1031–1044, Tulsa.

Blatt H. (1979) - Diagenetic processes in sandstones. *Soc. Econ. Paleont. Min.*, Sp. Publ., n. 26, pp. 141–157, Tulsa.

Bozorgnia F. (1964) - Microfacies and microorganisms of Paleozoic through Tertiary sediments of some parts of Iran. V. of 22 pp., 158 pl., 1 map, Ed. NIOC, Teheran.

Cavarretta G., Gianelli G. & Puxeddu M. (1984) - Formation of authigenic minerals and their use as indicators of the physicochemical parameters of the fluid in the Larderello–Travale geothermal field. *Econ. Geol. & Bull. Soc. Econ. Geol.*, v. 77, pp. 1–14.

Cleary W.J. & Conolly J.R. (1971) - Distribution and genesis of quartz in a piedmont – coastal plain environment. *Geol. Soc. Am. Bull.*, v. 82, pp. 2755–2766, Boulder.

Cleary W.J. & Conolly J.R. (1972) - Embayed quartz grains in soils and their significance. *Journ. Sedim. Petr.*, v. 42, pp. 899–904, Tulsa.

Collins J.S.H. & Morris S.F. (1975) - A new crab, *Costacopluma concava*, from the Upper Cretaceous of Nigeria. *Palaeontology*, v. 18, pp. 823–829, 1 pl., 1 fig., London.

Davies L.M. (1927) - The Ranikot Beds at Thal (North–West Frontier Prov. of India). *Quart. Journ. Geol. Soc.*, v. 83, n. 2, pp. 260–290, 5 pl., 7 fig., London.

De Mowbray T. (1983) - The genesis of lateral accretion deposits in recent intertidal mudflat channels, Solway Firth, Scotland. *Sedimentology*, v. 30, p. 425–435, Oxford.

Dickinson W.R. (1970) - Interpreting detrital modes of graywache and arkose. *Journ. Sedim. Petr.*, v. 40, pp. 695–707, Tulsa.

Dickinson W.R. & Suczek C.A. (1979) - Plate tectonics and sandstone composition. *Am. Ass. Petr. Geol. Bull.*, v. 63, pp. 2164–2172, Tulsa.

Dilley F.C. (1973) - Cretaceous Larger Foraminifera. In Hallam A. (Ed.) - Atlas of Palaeobiogeography, pp. 403–419, 12 fig., Elsevier, Amsterdam.

Dutta P.K. & Suttner L.J. (1986) - Alluvial sandstone composition and paleoclimate. II. Authigenic mineralogy. *Journ. Sedim. Petr.*, v. 56, pp. 346–358, Tulsa.

Fois E., Garzanti E. & Jadoul F. (in preparation) - Late Triassic–Early Jurassic sedimentary evolution in the Zanskar Tethys Himalaya (Ladakh, India). *Riv. Ital. Paleont. Strat.*, Milano.

Folk R. L. (1980) - Petrology of sedimentary rocks. Hemphill Publ. Co., 182 pp., Austin.

Franzinelli E. & Potter P.E. (1983) - Petrology, chemistry and texture of modern river sands, Amazon river system. *Journ. Geol.*, v. 91, pp. 23–39, Chicago.

Frey M. (1970) - The step from diagenesis to metamorphism in pelitic rocks during alpine orogenesis. *Sedimentology*, v. 15, pp. 261–279, Oxford.

Frey M., Hunziker J.C., Roggwiller P. & Schindler C. (1973) - Progressive niedriggradige Metamorphose glaukonitführender Horizonte in den helvetischen Alpen der Ostschweiz. *Contr. Min. Petrol.*, v. 39, pp. 185–218, Heidelberg.

Friedman G.M. (1967) - Dynamic processes and statistical parameters compared for size frequency distribution of beach and river sands. *Journ. Sedim. Petr.*, v. 37, pp. 327–354, Tulsa.

Friedman G.M. (1979) - Differences in size distributions of populations of particles among sands of various origins. *Sedimentology*, v. 26, pp. 3–32, Oxford.

Fuchs G. (1979) - On the geology of western Ladakh. *Jb. Geol. Bundesanst.*, v. 122, n. 2, pp. 513–540, Wien.

Fuchs G. (1982) - The geology of western Zanskar. *Jb. Geol. Bundesanst.*, v. 125, n. 1, pp. 1–50, Wien.

Fuchs G. (1986) - The geology of the Markha–Khurnak region in Ladakh (India). *Jb. Geol. Bundesanst.*, v. 128, n. 3, pp. 403–437, Wien.

Füchtbauer H. (1984) - Sediments and sedimentary rocks. Pt. II: Sedimentary petrology. V. of 464 pp., E. Schweizerbart'sche Verlagsbuchandlung, Stuttgart.

Gaetani M., Casnedi R., Fois E., Garzanti E., Jadoul F., Nicora A. & Tintori A. (1985a) - Stratigraphy of the Tethys Himalaya in Zanskar, Ladakh (Initial report). *Riv. Ital. Paleont. Strat.*, v. 91, n. 4, pp. 443–478, 16 fig., Milano.

Gaetani M., Garzanti E. & Jadoul F. (1985b) - Main structural elements of Zanskar, NW Himalaya (India). *Rend. Soc. Geol. It.*, v. 8, pp. 3–8, 2 fig., Roma.

Gaetani M., Nicora A. & Premoli Silva I. (1980) - Uppermost Cretaceous and Paleocene in the Zanskar range (Ladakh – Himalaya). *Riv. Ital. Paleont. Strat.*, v. 86, n. 1, pp. 127–166, 9 pl., 6 fig., Milano.

Gaetani M., Nicora A., Premoli Silva I., Fois E., Garzanti E. & Tintori A. (1983) - Upper Cretaceous and Paleocene in Zanskar range (NW Himalaya). *Riv. Ital. Paleont. Strat.*, v. 89, n. 1, pp. 81–118, 4 pl., 6 fig., Milano.

Gansser A. (1964) - Geology of the Himalayas. V. of 289 pp., Wiley Interscience Publ., London.
Garzanti E. (1986) - Storia sedimentaria del margine settentrionale della placca indiana (Tethys Himalaya, Ladakh, India). Tesi di Dottorato, Università di Milano.
Garzanti E., Baud A. & Mascle G. (in preparation) - Sedimentary record of the northward flight of India and its collision with Eurasia (NW Himalaya, India).
Garzanti E., Casnedi R. & Jadoul F. (1986) - Sedimentary evidence of a Cambro–Ordovician orogenic event in the Northwestern Himalaya. *Sedim. Geol.*, v. 48, pp. 237–265, Amsterdam.
Goldbery R. (1979) - A textural inversion phenomenon within Lower Jurassic red beds of the Ardon Formation, Makhtesh Ramon (Israel). *Journ. Sedim. Petr.*, v. 49, pp. 891–900, Tulsa.
Hasson P.F. (1985) - New observations on the biostratigraphy of the Saudi Arabian Umm er Radhuma Formation (Paleocene) and its correlation with neighboring regions. *Micropaleont.*, v. 31, n. 4, pp. 335–364, 8 pl., 8 fig., New York.
Hedberg H.D. (Ed.) (1976) - International Stratigraphic Guide. A guide to stratigraphic classification, terminology and procedure. V. of 200 pp., 14 fig., Wiley, New York.
Henson F.R.S. (1948) - Larger imperforate Foraminifera of South–Western Asia. V. of 127 pp., 16 pl., 16 fig., Ed. *Brit. Mus. (Nat. Hist.)*, London.
Hottinger L. (1960a) - Recherches sur les *Alvéolines* du Paléocène et de l'Eocène. *Schw. Palaeont. Abhandl.*, v. 75/76, Texte (I): 144 pp., 1 tab., 117 fig.; Atlas (II): 18 pl., Basel.
Hottinger L. (1960b) - Über paleocaene und eocaene Alveolinen. *Ecl. Geol. Helv.*, v. 53, n. 1, pp. 265–284, 21 pl., 1 tab., 3 fig., Basel.
Hottinger L. (1966) - Foraminifères rotaliformes et Orbitoides du Sénonien inférieur pyrénéen. *Ecl. Geol. Helv.*, v. 59, n. 1, pp. 277–302, 6 pl., 11 fig., Basel.
Hottinger L. (1973) - Selected Paleogene Larger Foraminifera. In Hallam A. (Ed.) - Atlas of Palaeobiogeography, pp. 443–452, 6 fig., Elsevier, Amsterdam.
Hottinger L. (1980) - Rotaliid Foraminifera. *Schw. Palaeont. Abhandl.*, v. 101, 154 pp., 66 pl., 57 fig., Basel.
Johnsson M.J., Stallard R.F. & Meade R.H. (1986) - First cycle quartz arenites in the Orinoco River basin, Colombia and Venezuela. 1986 SEPM Midyear Meeting, Raleigh, Abstract.
Klootwijk C. (1979) - A review of paleomagnetic data from the Indo–Pakistani fragment of Gondwanaland. In Farah A. & De Jong K. (Eds.) - Geodynamics of Pakistan. *Geol. Surv. Pakistan*, pp. 41–80, Quetta.
Kossovskaya A.G. & Shutov V.D. (1970) - Main aspects of the epigenesis problem. *Sedimentology*, v. 15, pp. 11–40, Oxford.
Kureshy A.A. (1977) - The Cretaceous larger foraminiferal biostratigraphy of Pakistan. *Journ. Geol. Soc. India*, v. 18, pp. 662–667, Bombay.
Kureshy A.A. (1978) - Tertiary larger foraminiferal zones of Pakistan. *Rev. Esp. Micropaleont.*, v. 10, n. 3, pp. 467–483, 8 fig., Madrid.
Latif M.A. (1976) - Stratigraphy and Micropaleontology of the Galis Group of Hazara, Pakistan. *Geol. Bull. Panjab Univ.*, n. 13, 65 pp., 16 pl., 4 fig., Lahore.
Lehmann R.v. (1961) - Strukturanalyse einiger Gattungen der Subfamilie *Orbitolininae*. *Ecl. Geol. Helv.*, v. 54, n. 2, pp. 599–667, 14 pl., 49 fig., Basel.
Mack G.H. (1978) - The survivability of labile light–mineral grains in fluvial, aeolian and littoral marine environments: the Permian Cutler and Cedar Mesa Formations, Moab, Utah. *Sedimentology*, v. 25, pp. 587–604, Oxford.
Mazzullo J. (1986) - Sources and provinces of late Quaternary sand on the East Texas–Loui-

siana continental shelf. *Geol. Soc. Am. Bull.*, v. 97, pp. 638–647, Boulder.

McCubbin D.G. (1982) - Barrier–island and strand–plain facies. *Am. Ass. Petr. Geol., Mem.* n. 31, pp. 247–279, Tulsa.

Morellet M.L. (in Douvillé H.) (1916) - Le Crétacé et l'Eocène du Tibet Central. *Palaeont. Indica*, N.S., v. 5, mem. 3, pp. 1–52, 16 pl., 21 fig., Calcutta.

Moslow T.F. (1984) - Depositional models of shelf and shoreline sandstones. *Am. Ass. Petr. Geol.* Course note series # 27, 102 pp., Tulsa.

Nagappa Y. (1959) - Foraminiferal biostratigraphy of Cretaceous – Eocene succession in the India–Pakistan–Burma region. *Micropaleont.*, v. 5, n. 2, pp. 145–192, 11 pl., 11 fig., New York.

Odom I.E. (1975) - Feldspar–grain size relations in Cambrian arenites, upper Mississippi valley. *Journ. Sedim. Petr.*, v. 45, pp. 636–650, Tulsa.

Odom I.E., Doe T.W. & Dott R.H. (1976) - Nature of feldspar–grain size relations in some quartz–rich sandstones. *Journ. Sedim. Petr.*, v. 46, pp. 862–870, Tulsa.

Patriat P. & Achache J. (1984) - India–Eurasia collision chronology has implications for crustal shortening and driving mechanism of plates. *Nature*, v. 311, pp. 615–621, London.

Pegasus (Ed.) (1983) - Ladakh–Zanskar map, scale 1:350.000, Zürich.

Pitman W.C. (1978) - Relationship between sea–level change and stratigraphic sequences. *Geol. Soc. Am. Bull.*, v. 89, pp. 1389–1403, Boulder.

Pitman W.C. & Golovchenko X. (1983) - The effect of sealevel change on the shelfedge and slope of passive margins. *Soc. Econ. Paleont. Min.*, Sp. Publ., n. 33, pp. 41–58, Tulsa.

Potter P.E. (1978) - Petrology and chemistry of modern big river sands. *Journ. Geol.*, v. 86, pp. 423–449, Chicago.

Potter P.E. (1986) - South America and a few grains of sand. Part I: Beach sands. *Journ. Geol.*, v. 94, pp. 301–319, Chicago.

Premoli Silva I. (1970) - The Cretaceous and Paleocene microfaunas from North–East Afghanistan. In Desio A. (Ed.) - Fossils of North–east Afghanistan. *Italian Exp. Karakorum and Hindu–Kush, Scient. Rep.*, v. 4, n. 2, pp. 119–160, 8 pl., 1 fig., Ed. E.J. Brill, Leiden.

Reinson G.E. (1984) - Barrier–island and associated strand–plain systems. In Walker R. (Ed.) - Facies models. Geoscience Canada Reprint Series, pp. 119–140, Toronto.

Sampò M. (1969) - Microfacies and microfossils of the Zagros Area, Southwestern Iran (From Pre–Permian to Miocene). V. of 87 pp., 105 pl., 6 fig., Ed. E. J. Brill, Leiden.

Savostin L.A., Sibuet J.C., Zonenshain L.P., Le Pichon X. & Roulet M.R. (1986) - Kinematic evolution of the Tethys belt from the Atlantic ocean to the Pamirs since the Triassic. In Aubouin J., Le Pichon X. & Monin A. (Eds.) - Evolution of the Tethys. *Tectonophysics*, v. 123, pp. 1–35, Amsterdam.

Schaub H. (1981) - Nummulites et Assilines de la Téthys paléogène. Taxinomie, phylogénèse et biostratigraphie. *Schw. Palaeont. Abhandl.*, v. 104, 238 pp., 18 pl., 116 fig., Basel.

Schiffman P., Elders W.A., Williams A.E., McDowell S.D. & Bird D.K. (1984) - Active metasomatism in the Cerro Prieto geothermal system, Baja California, Mexico: a telescoped low–pressure, low–temperature metamorphic facies series. *Geology*, v. 12, pp. 12–15, Boulder.

Schmidt V. & McDonald D.A. (1979) - The role of secondary porosity in the course of sandstone diagenesis. *Soc. Econ. Paleont. Min.*, Sp. Publ., n. 26, pp. 175–207, Tulsa.

Schwab F.L. (1976) - Modern and ancient sedimentary basins: comparative accumulation rates. *Geology*, v. 4, pp. 723–727, Boulder.

Siever R. (1959) - Petrology and geochemistry of silica cementation in some Pennsylvanian sandstones. *Soc. Econ. Paleont. Min.*, Sp. Publ., n. 7, pp. 59–79, Tulsa.

Smout A.H. (1954) - Lower Tertiary Foraminifera of the Qatar Peninsula. V. of 97 pp., 15 pl., 44 fig., Ed. *Brit. Mus. (Nat. Hist.)*, London.

Speed R.C. & Sleep N.H. (1982) - Antler orogeny and foreland basin: a model. *Geol. Soc. Am. Bull.*, v. 93, pp. 815–828, Boulder.

Srivastava R.K. (1983) - Temporal status of alkaline rocks of Deccan volcanic province. *Geol. Mag.*, v. 120, n. 3, pp. 303–304, London.

Stockmal G.S., Beaumont C. & Boutilier R. (1986) - Geodynamic models of convergent margin tectonics: transition from rifted margin to overthrust belt and consequences for foreland basin development. *Am. Ass. Petr. Geol. Bull.*, v. 70, pp. 181–190, Tulsa.

Stonecipher S.A., Winn R.D. & Bishop M.G. (1984) - Diagenesis of the Frontier Formation, Moxa Arch: a function of sandstone geometry, texture and composition, and fluid flux. *Am. Ass. Petr. Geol., Mem.* n. 37, pp. 289–316, Tulsa.

Suttner L.J., Basu A. & Mack G.H. (1981) - Climate and origin of quartzarenites. *Journ. Sedim. Petr.*, v. 51, pp. 1235–1246, Tulsa.

Suttner L.J. & Dutta P.K. (1986) - Alluvial sandstone composition and paleoclimate: I. Framework mineralogy. *Journ. Sedim. Petr.*, v. 56, pp. 329–345, Tulsa.

Taira A. & Scholle P.A. (1979) - Origin of bimodal sands in some modern environments. *Journ. Sedim. Petr.*, v. 49, pp. 777–786, Tulsa.

Tibetan Scientific Expedition Team Academia Sinica (1975) - A report of a scientific expedition in the Mount Jolmo Lungma region (1966–1968), n. 2, pp. 425–457, 12 pl., Peking.

Vail P.R., Hardenbol J. & Todd R.G. (1984) - Jurassic unconformities, chronostratigraphy and sea level changes from seismic stratigraphy and biostratigraphy. *Am. Ass. Petr. Geol., Mem.* n. 36, pp. 129–144, Tulsa.

Vail P.R., Mitchum R.M. & Thompson S. (1977) - Global cycles of relative changes in sea level. *Am. Ass. Petr. Geol., Mem.* n. 26, pp. 83–97, Tulsa.

Vail P.R. & Todd R.G. (1981) - Northern North Sea Jurassic unconformities, chronostratigraphy and sea–level changes from seismic stratigraphy. In Illing L. & Hobson G. (Eds.) - Petroleum geology of the continental shelf of the northwest Europe, pp. 216–235, Heyden, Inst. Petroleum, London.

Visher G.S. (1969) - Grain size distributions and depositional processes. *Journ. Sedim. Petr.*, v. 39, pp. 1074–1106, Tulsa.

Voll G. (1982) - Bewegung von Korngrenzen in Gesteinen. Vortrag, DFG "Gesteinskinetic–Sitzung", 24.4.82, Tübingen.

Vredenburg W.E. (1916) - *Flemingostrea*, an eastern group of Upper Cretaceous and Eocene *Ostreidae:* with descriptions of two new species. *Rec. Geol. Surv. India*, v. 47, pp. 196–203, 4 pl., Calcutta.

Wannier M. (1983) - Evolution, biostratigraphie et systématique des *Siderolitinae* (Foraminifères). *Rev. Esp. Micropaleont.*, v. 15, n. 1, pp. 5–37, 7 pl., 8 fig., Madrid.

Weimer R.J., Porter K.W. & Land C.B. (1985) - Depositional modeling of detrital rocks. *Soc. Econ. Paleont. Min.*, Core workshop #8, 252 pp., Tulsa.

Winn R.D., Stonecipher S.A. & Bishop M.G. (1984) - Sorting and wave abrasion: controls on composition and diagenesis in the Lower Frontier sandstones, southwestern Wyoming. *Am. Ass. Petr. Geol. Bull.*, v. 68, pp. 269–284, Tulsa.

PLATE 32

Fig. 1 – Bioclastic packstone with *Omphalocyclus macroporus* (Lamarck). Dibling section, Marpo Limestone; sample HZ 352; x 6.

Fig. 2 – Bioclastic packstone with *Goupillaudina* sp. Same sample of fig. 1; x 20.

Fig. 3 – Bioclastic packstone with *Siderolites calcitrapoides* Lamarck. Dibling section, Marpo Limestone; sample HZ 359; x 5.

Fig. 4 – Bioclastic packstone with *Omphalocyclus macroporus* (Lamarck) and *Siderolites calcitrapoides* Lamarck. Dibling section, Marpo Limestone; sample HZ 360; x 5.

Fig. 5 – Bioclastic packstone with *Clypeina* cf. *merienda* Elliott. Marpo section, Dibling Limestone; sample HZ 307; x 20.

Fig. 6 – Bioclastic packstone with a) *Furcoporella diplopora* Pia and b) *Clypeina* cf. *merienda* Elliott. Same sample of fig. 5; x 30.

Fig. 7 – Bioclastic packstone with *Clypeina* cf. *merienda* Elliott and rotaliids. Same sample of fig. 5; x 12.

Fig. 8 – Bioclastic packstone with a) *Ovulites* cf. *kangpensis* Yu–Jing and rotaliids. Same sample of fig. 5; x 10.

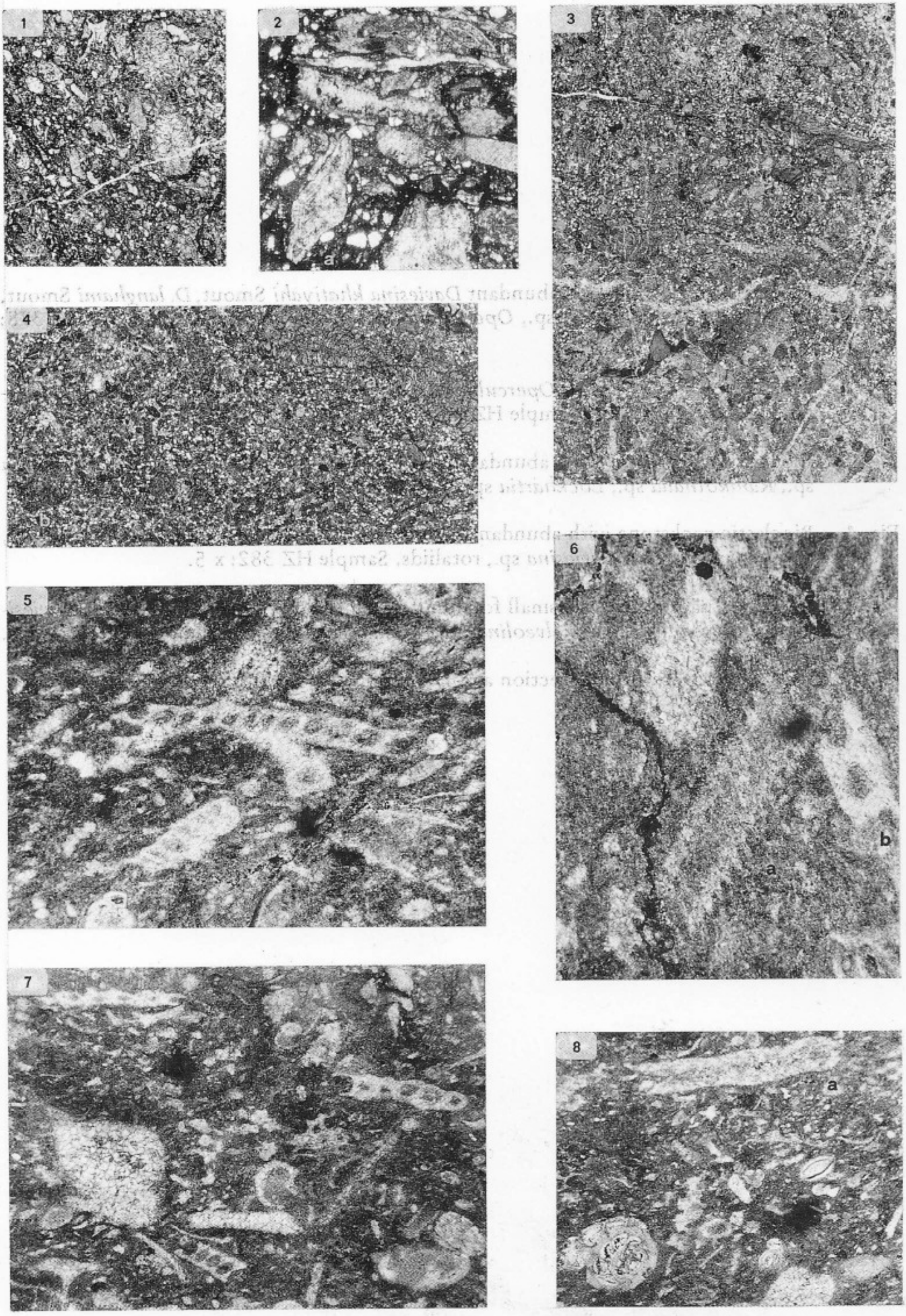

PLATE 33

Fig. 1 – Bioclastic packstone with abundant *Daviesina khatiyahi* Smout, *D. langhami* Smout, *Daviesina* sp., *Lockhartia* sp., *Operculina* sp., *Sphaerogypsina* sp. Sample HZ 378; x 5.

Fig. 2 – Bioclastic packstone with *Operculina* sp., *Lockhartia* sp., *Daviesina* sp., small foraminifera, *Textulariidae*. Sample HZ 378; x 5.

Fig. 3 – Bioclastic packstone with abundant small foraminifera, *Daviesina* sp., *Operculina* sp., *Ranikothalia* sp., *Lockhartia* sp. Sample HZ 383; x 5.

Fig. 4 – Bioclastic packstone with abundant small foraminifera, miliolids, *Ataxophragmiidae*, *Sphaerogypsina* sp., *Daviesina* sp., rotaliids. Sample HZ 382; x 5.

Fig. 5 – Bioclastic packstone with small foraminifera, miliolids, *Sphaerogypsina* sp., *Daviesina* sp., *Fasciolites (Glomalveolina)* cf. *primaeva* (Reichel). Sample HZ 382; x 5.

All samples from Dibling section and Dibling Limestone, Lithozone *A*.

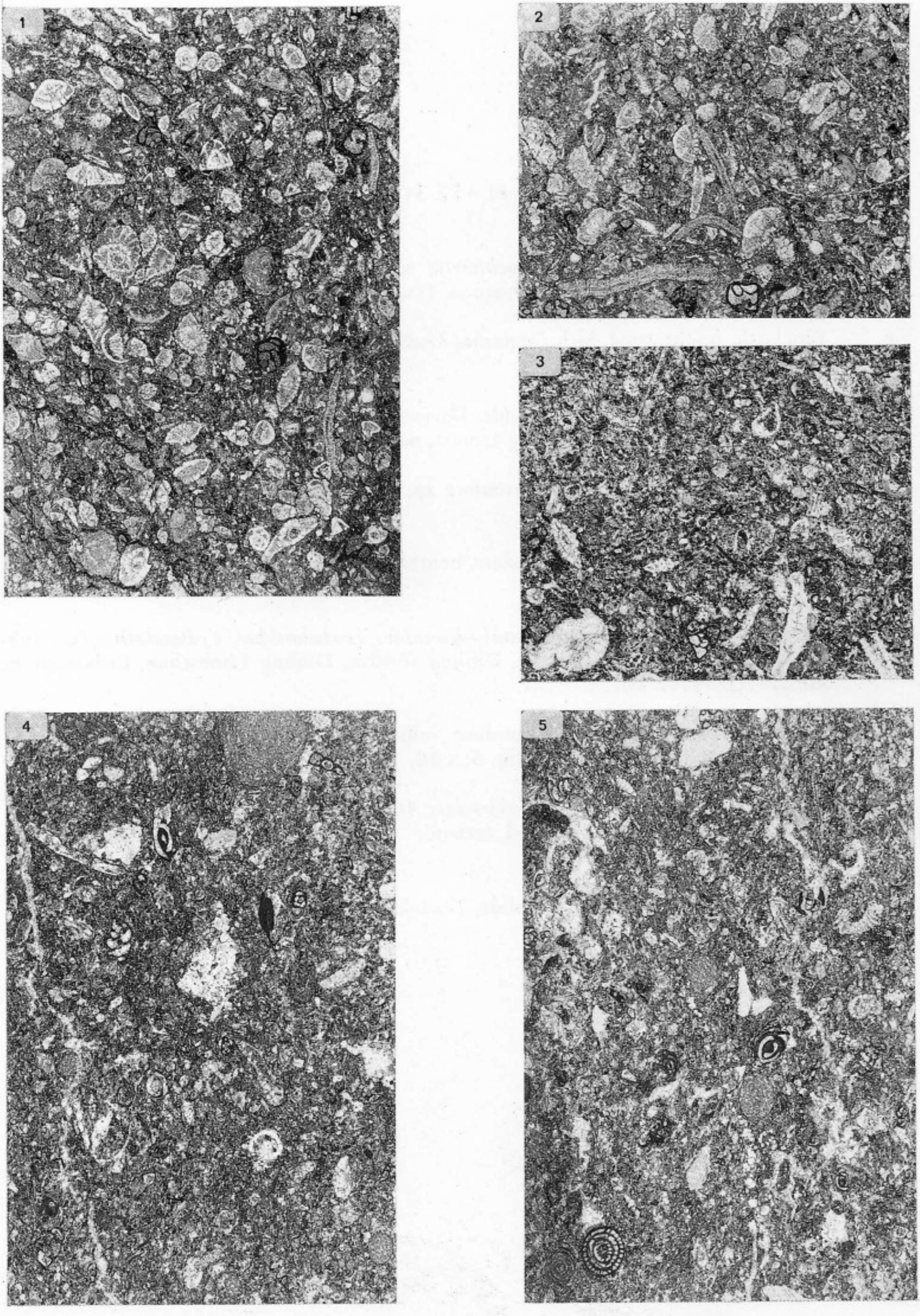
1
2
3
4
5

PLATE 34

Fig. 1 – Bioclastic wackestone with *Lockhartia* sp., *Daviesina* sp., *Operculina* sp. Marpo section, Dibling Limestone, Lithozone *A;* sample HZ 311; x 16.

Fig. 2 – Bioclastic wackestone with *Daviesina khatiyahi* Smout, fragmented rotaliids. Same sample of fig. 1; x 8.

Fig. 3 – Bioclastic packstone with rotaliids, *Daviesina danieli* Smout, *Textulariidae, Gavelinella* sp. Dibling section, Dibling Limestone, Lithozone *B;* sample HZ 375; x 8.

Fig. 4 – Bioclastic packstone with *Operculina* sp., rotaliids and small foraminifera. Same sample of fig. 3; x 16.

Fig. 5 – Bioclastic packstone with abundant benthic foraminifera, miliolids, rotaliids. Same sample of fig. 3; x 10.

Fig. 6 – Bioclastic packstone with *Ataxophragmiidae, Textulariidae,* a) *Fasciolites (G.) subtilis* (Hottinger), *Fasciolites* sp. Dibling section, Dibling Limestone, Lithozone *B;* sample HZ 397; x 10.

Fig. 7 – Bioclastic packstone with abundant miliolids, *Ataxophragmiidae*, rotaliids and *Orbitolites* sp. Same sample of fig. 6; x 10.

Fig. 8 – Bioclastic packstone with *Textulariidae, Ataxophragmiidae,* miliolids and *Lockhartia* sp. Dibling section, second tectonic slab, Dibling Limestone, Lithozone *B*; sample HZ 419; x 10.

Fig. 9 – Bioclastic packstone with miliolids, *Textulariidae, Ataxophragmiidae, Valvulinidae.* Same sample of fig. 8; x 10.

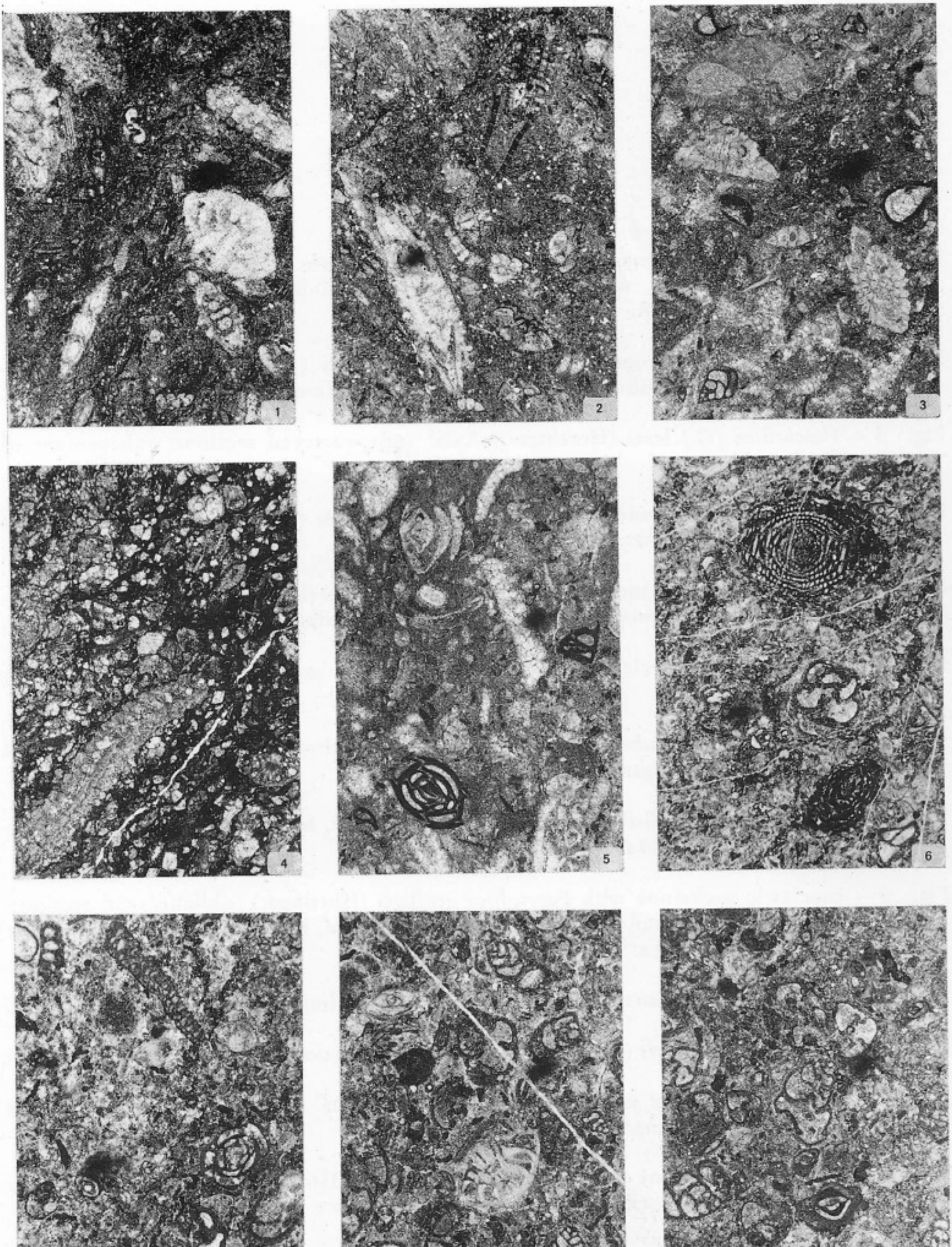
1
2
3
4
5
6
7
8
9

PLATE 35

Fig. 1 – Bioclastic wackestone with *Fasciolites (G.) subtilis* (Hottinger), *Orbitolites* sp., *Ataxophragmiidae*, miliolids. Dibling section, Dibling Limestone, Lithozone *B*; sample HZ 400; x 8.

Fig. 2 – Bioclastic wackestone with *Fasciolites (G.) levis* (Hottinger), miliolids, *Ataxophragmiidae* and abundant other small foraminifera. Same sample of fig. 1; x 7.

Fig. 3 – *Fasciolites (G.) levis* (Hottinger). Axial and equatorial sections; enlargement of fig. 2, x 20.

Fig. 4 – Bioclastic wackestone with a) *Fasciolites (G.) levis* (Hottinger); b) *F. (G.) subtilis* (Hottinger), miliolids. Same sample of fig. 1; x 10.

Fig. 5 – Bioclastic wackestone with *Fasciolites (G.) subtilis* (Hottinger), miliolids, *Textulariidae, Ataxophragmiidae* and other small foraminifera. Same sample of fig. 1; x 7.

Fig. 6 – *Fasciolites (G.) levis* (Hottinger). Oblique/axial section; enlargement of fig. 2, x 20.

Fig. 7 – *Fasciolites (G.) subtilis* (Hottinger). Axial section. Miliolids and other small foraminifera; enlargement of fig. 5, x 15.

Fig. 8 – *Fasciolites (G.) subtilis* (Hottinger). Axial section. Marpo section, Dibling Limestone, Lithozone *B*; sample HZ 324; x 30.

Fig. 9 – Bioclastic packstone with *Fasciolites avellana* (Hottinger) (oblique/axial section), *Lockhartia* sp., small foraminifera. Dibling section, Dibling Limestone, Lithozone *B*; sample HZ 401; x 9.

Fig. 10 – *Fasciolites* cf. *varians* (Hottinger). Equatorial section. Same sample of fig. 9; x 18.

Fig. 11 – *Fasciolites (G.) levis* (Hottinger). Oblique/axial section. Same sample of fig. 8; x 20.

Fig. 12 – *Fasciolites avellana aurignacensis* (Hottinger). Axial section. *Ovulites* cf. *elongata* Lamarck. Same sample of fig. 9; x 25.

Fig. 13 – Bioclastic packstone with abundant udoteacean *Algae* (a) *Halymeda* sp., *Ovulites* cf. *elongata* Lamarck and small foraminifera. Same sample of fig. 9; x 10.

Fig. 14 – Bioclastic packstone with small foraminifera and *Orbitolites* sp. Same sample of fig. 8; x 15.

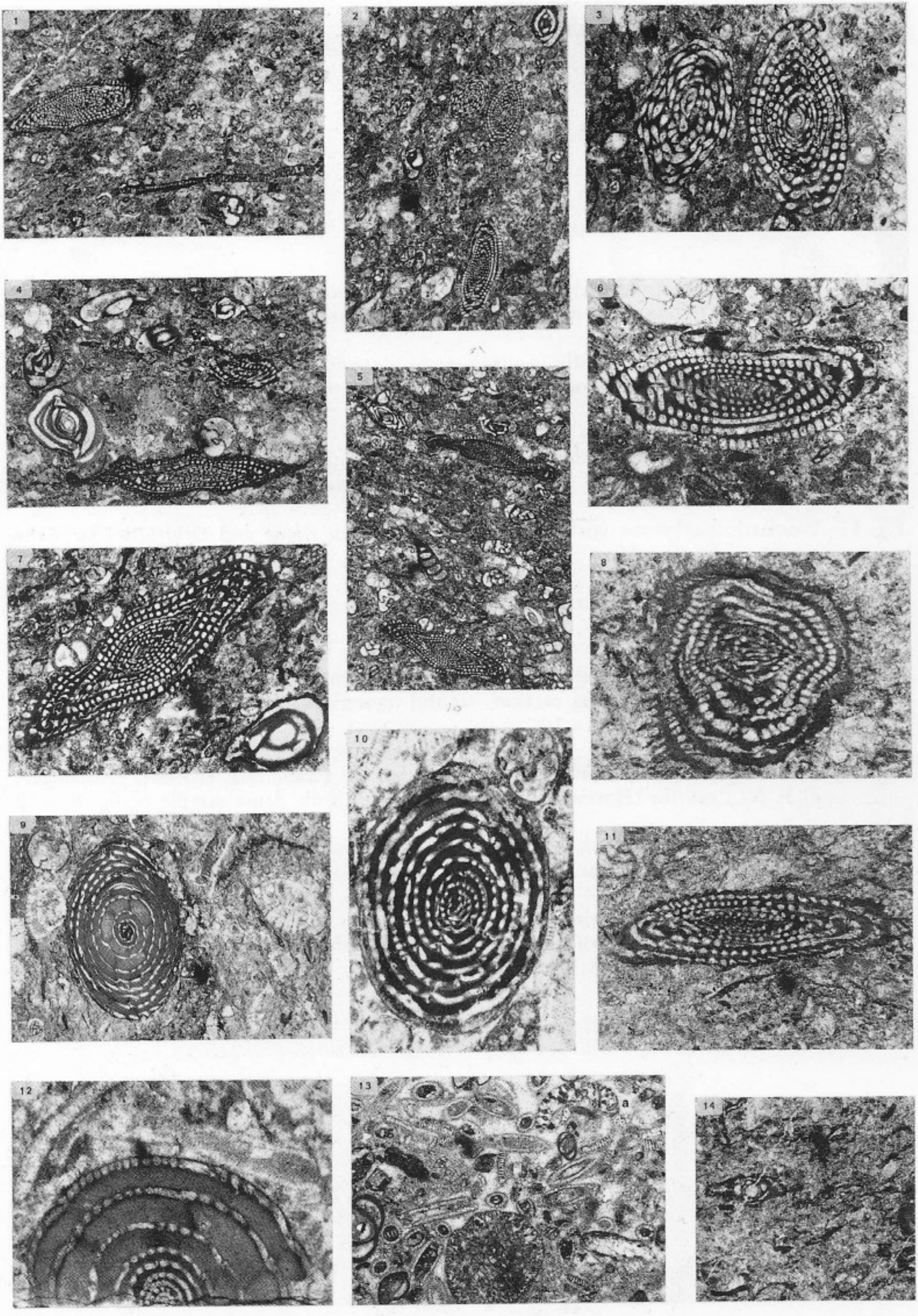
1
2
3
4
5
6
7
8
9
10
11
12
13
a
14

PLATE 36

Fig. 1 – Bioclastic packstone with: a) *Ovulites* cf. *margaritula* (Lamarck); b) *O.* cf. *elongata* Lamarck. Dibling section, Dibling Limestone, Lithozone *B*; sample HZ 401; x 10.

Fig. 2 – Bioclastic packstone with: a) *Halymeda* sp. and abundant *Ovulites* cf. *elongata* Lamarck. Dibling section, Dibling Limestone, uppermost part of Lithozone *B*; sample HZ 402; x 12.

Fig. 3 – Bioclastic packstone with: a) *Halymeda* aff. *lingulata* Yu–Jing; b) *Ovulites* cf. *margaritula* (Lamarck); c) *O.* cf. *elongata* Lamarck. Same sample of fig. 2; x 10.

Fig. 4 – Bioclastic packstone with remains of udoteacean *Algae* and *Orbitolites* sp. Same sample of fig. 1; x 10.

Fig. 5 – *Fasciolites avellana* (Hottinger). Oblique/axial section; enlargement of fig. 9 in Plate 35, x 17.

Fig. 6 – Bioclastic packstone with rotaliids, miliolids, small foraminifera, *Fasciolites (G.) levis* (Hottinger). Dibling section, second tectonic slab, Dibling Limestone, Lithozone *B*; sample HZ 417; x 10.

Fig. 7 – Bioclastic packstone with: a) *Orbitolites* sp.; b) *Fasciolites (G.) levis* (Hottinger); c) *F. (G.) subtilis* (Hottinger) and small foraminifera. Same sample of fig. 6; x 10.

Fig. 8 – Bioclastic packstone with: a) *Fasciolites avellana* (Hottinger); b) *F. (G.) subtilis* (Hottinger) and small foraminifera. Same sample of fig. 6; x 10.

Fig. 9 – Bioclastic packstone with small foraminifera: a) *Fasciolites cucumiformis* (Hottinger); b) *F. (G.) subtilis* (Hottinger), highly deformed. Marpo section, Dibling Limestone, Lithozone *B*; sample HZ 324; x 10.

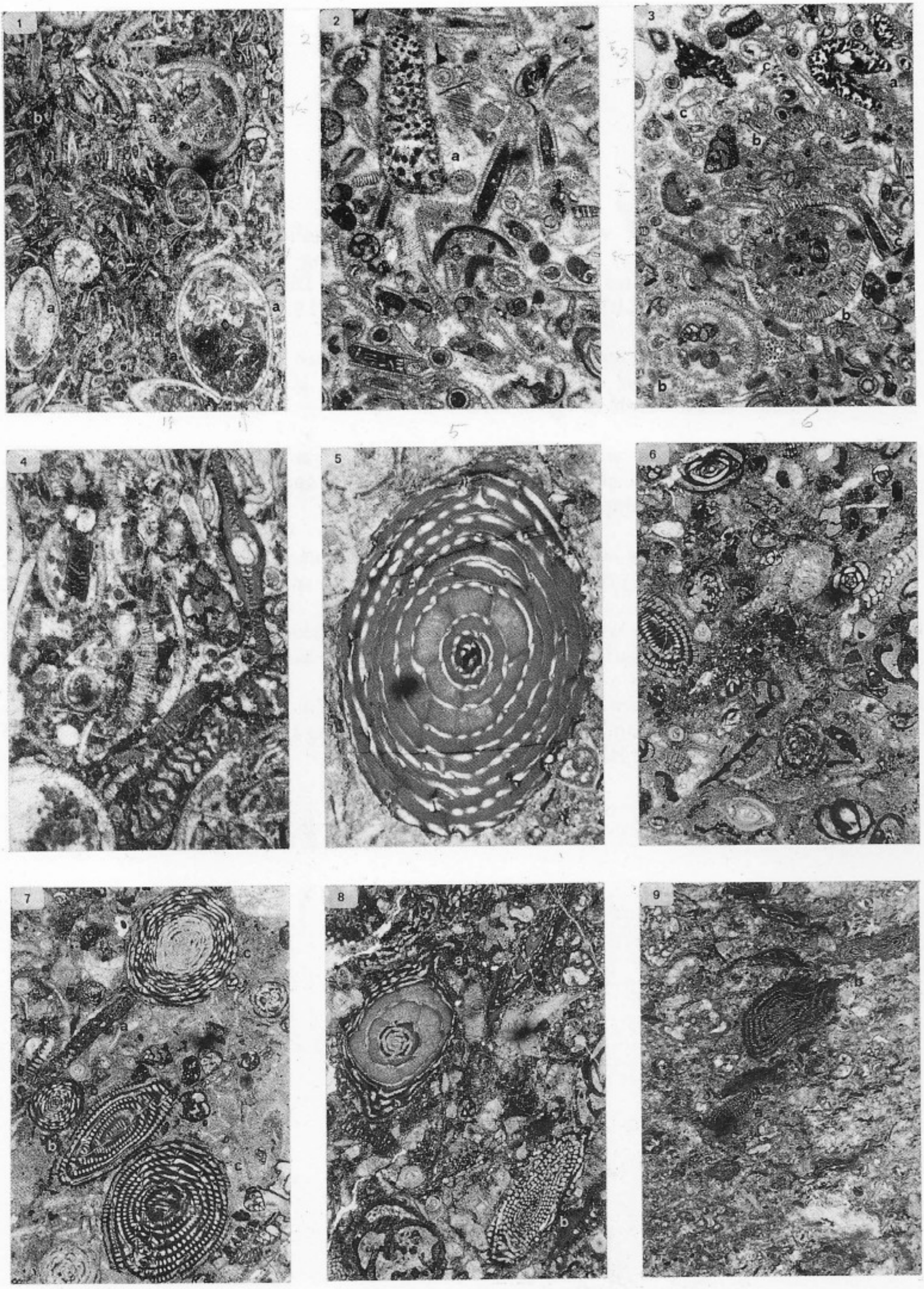

PLATE 37

Fig. 1 – Bioclastic packstone with small foraminifera (miliolids, *Textulariidae*), abundant udoteacean *Algae* (a) *Halymeda lingulata* Yu–Jing; b) *Ovulites* cf. *elongata* Lamarck) and *Fasciolites* gr. *ellipsoidalis* (Schwager). Dibling section, Dibling Limestone, upper part of Lithozone *B*; sample HZ 402; x 15.

Fig. 2 – Bioclastic packstone mostly dominated by udoteacean *Algae*: a) *Halymeda lingulata* Yu–Jing; b) *Ovulites* cf. *elongata* Lamarck; c) *O.* cf. *margaritula* (Lamarck) and miliolids. Same sample of fig. 1; x 15.

Fig. 3 – Bioclastic packstone with abundant udoteacean *Algae* (a) *Halymeda lingulata* Yu–Jing; b) *Ovulites* cf. *elongata* Lamarck), miliolids and *Fasciolites (G.)* cf. *subtilis* (Hottinger). Same sample of fig. 1; x 10.

Fig. 4 – Bioclastic packstone with: a) *Halymeda* aff. *lingulata* Yu–Jing; b) *Ovulites* cf. *elongata* Lamarck; c) *Halymeda* sp. and *Orbitolites* sp. Same sample of fig. 1; x 15.

Fig. 5 – Bioclastic packstone with dominant a) *Ovulites* cf. *elongata* Lamarck; subordinated b) *Halymeda* aff. *lingulata* Yu–Jing, miliolids. Same sample of fig. 1; x 15.

Fig. 6 – Bioclastic packstone with: a) *Halymeda lingulata* Yu–Jing, miliolids, small foraminifera. Dibling section, second tectonic slab, Dibling Limestone, uppermost part of Lithozone *B*; sample HZ 414; x 25.

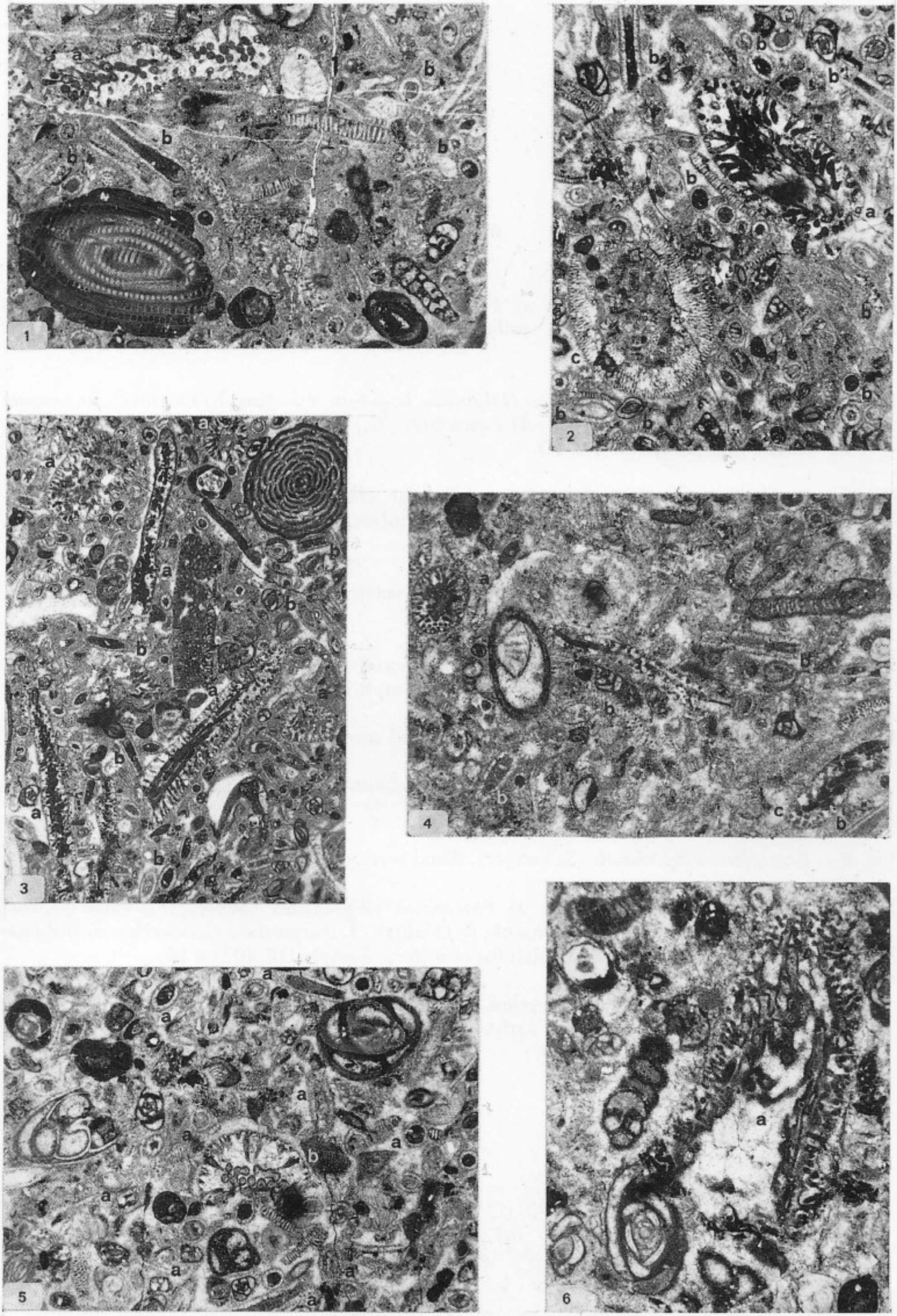
1
2
3
4
5
6

PLATE 38

Fig. 1 – Bioclastic packstone with: a) *Fasciolites (G.) subtilis* (Hottinger); b) *Fasciolites cucumiformis* (Hottinger), miliolids, *Textulariidae, Ataxophragmiidae.* Sample HZ 414; x 12.

Fig. 2 – Bioclastic packstone with: a) *Halymeda lingulata* Yu–Jing; b) *Ovulites* cf. *elongata* Lamarck; c) *Orbitolites* sp.; d) *Fasciolites (G.) levis* (Hottinger), miliolids, *Textulariidae.* Sample HZ 402; x 30.

Fig. 3 – Bioclastic packstone with: a) *Fasciolites* gr. *ellipsoidalis* (Schwager); b) *Ovulites* cf. *elongata* Lamarck; c) *Ovulites* sp., miliolids, *Textulariidae, Ataxophragmiidae.* Sample HZ 402; x 15.

Fig. 4 – a) *Fasciolites (G.) levis* (Hottinger), axial section; b) *Ovulites* cf. *elongata* Lamarck. Sample HZ 402; x 40.

Fig. 5 – a) *Fasciolites lepidula* (Hottinger), equatorial section; b) *Ovulites* cf. *elongata* Lamarck; c) *Ovulites* sp.; d) *Halymeda* sp. Sample HZ 402; x 30.

Fig. 6 – *Fasciolites* gr. *ellipsoidalis* (Schwager), axial section. Sample HZ 402; x 30.

Fig. 7 – Bioclastic packstone with *Fasciolites ellipsoidalis* (Schwager) and miliolids. Sample HZ 408; x 8.

Fig. 8 – *Fasciolites ellipsoidalis* (Schwager). Axial section; enlargement of fig. 7, x 16.

Fig. 9 – Bioclastic packstone with: a) *Fasciolites ellipsoidalis* (Schwager), axial section; b) *Ovulites* cf. *elongata* Lamarck; c) *Ovulites* cf. *margaritula* (Lamarck); d) *Halymeda lingulata* Yu–Jing and small foraminifera. Sample HZ 402; x 16.

All samples from Dibling section and Dibling Limestone. Samples HZ 414, HZ 402 from the uppermost part of Lithozone *B*; sample HZ 408 from Lithozone C.

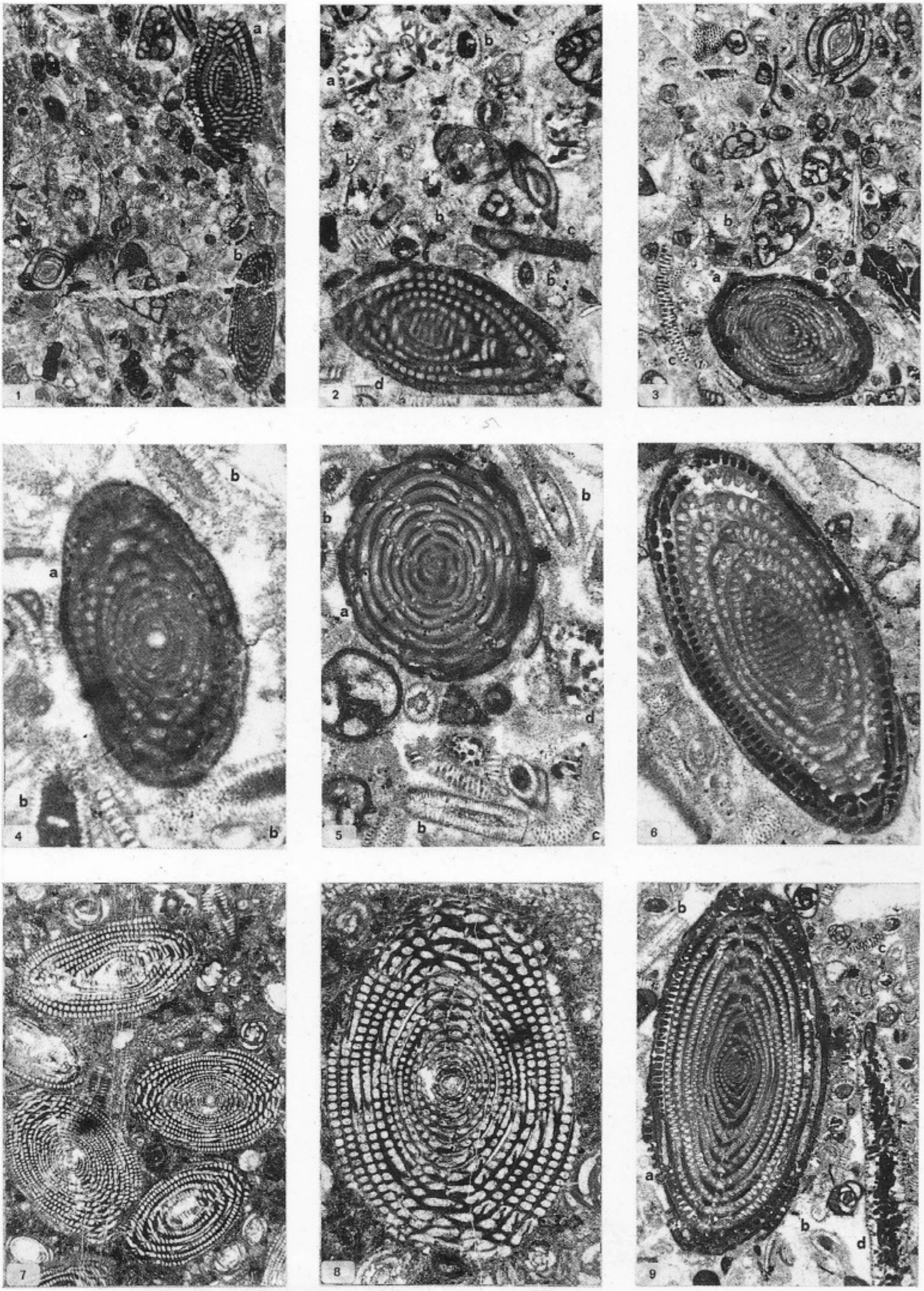
1
a
b
2
a
b
c
d
3
a
b
c
4
a
b
5
a
b
c
d
6
7
8
9
a
b
c
d